Julijana Simonović

MULTY-PARAMETRIC ANALYSIS OF COMPLEX HYBRID SYSTEMS DYNAMICS UNDER EXTERNAL EXCITATION

Abstract. Based on the given conceptual models of real phenomena from the disparate scientific fields the main task of my nine-year research was to establish corresponding mathematical models with acceptable approximations and to give a satisfactory prediction of system dynamics behavior. The relationship of main variables has predominantly non-linear properties thus we use nonlinear analysis and Krylov-Bogoliubov-Mitropolsky method to obtain first asymptotic approximations of system dynamics behavior and to be able to study parameter changes influence analytically and numerically. The multi-mode mutual coupling and transition through resonant regimes of system dynamics were analyzed and explained. Since the number of contributed parameters was considerable the multi-parametric analysis was exploited to examine the synchronization of system parts with external periodic loading. The mathematical analogy between discrete and continuous systems dynamics was detected and used in disparate phenomena behavior description. Continuous mechanical system nonlinear coupling, nonlinear lattice of orthogonal chains of discrete material particles representing biological systems of zona pellucid, and population models of bone cell behavior were all analyzed by using the same mathematical formalism and mapping. The mathematical analogy was detected in time-domain of solutions for disparate natural phenomena so that the same dynamics behavior can be detected and explained.

Mathematics Subject Classification (2010): Primary: 70-99, 74-99, 70F35, 92C10, 74L10, 70Q05. Secondary: 70Exx, 70KXX, 74M05, 37H20, 34D20, 70K20, 34C23.

Keywords: conceptual model, phenomenological analogy, time-domain of the solution, passage through resonant regimes, amplitude/phase jumps, multi-mode coupling, multi-parametric analysis, synchronization, external periodic excitation.

Faculty of Mechanical Engineering, University of Nis, Serbia,
julijana.simonovic@masfak.ni.ac.rs

Contents

1. Introduction

Theory of Mihailo Petrović Alas, presented in two books [1–2], contains elements of mathematical phenomenology and phenomenological mapping. Both publications were published in Serbian and only a small number of his contemporaries were able to read and understand this theory. However, the modern scientific public can find several examples of theory explanation and application in the paper by Hedrih and Simonovic (2015). The idea of mathematical phenomenology of M. Petrović, was presented in his works entitled "Phenomenological Mapping" [2]. "Phenomenological Mapping" by M. Petrović Alas and his mathematical phenomenology and mathematical analogy can be considered to be the continuation of the ideas of Poincare's mapping. Like his teacher Poincare, Petrovic also accepted the approach of the mathematical transformations that can be used for analyzing the original system, often too complex, in a simpler way. The transformations are suitable as long as they preserve many properties of periodic and quasiperiodic orbits of the original system and has a lower-dimensional state space. This approach is especially useful for analyzing the non-linear dynamics of complex continuous dynamical systems.

Based on this theory it is possible to make integration of contemporary knowledge obtained in various areas of sciences and identify analogous dynamics and phenomena. Phenomenological mapping of phenomenon and models enables multiple system dynamics models of disparate nature to be described by a single mathematical model. The well-known example is mathematical analogy of electrical circuit, so-calld electro-mechanics analogy, consisting of a resistor, an inductor, and a capacitor, connected in series or in parallel with simple harmonic oscillator. Rašković [3] gave a series of examples for electromechanical mathematically analogous

vibration systems mathematically described and solved for free vibrations. By using idea from [1-2], in the paper [4] an analogy between vector models of stress state, strain state and model of the state of the body mass inertia moments were presented and used for explanation in possible phenomenological mapping of these different kind states.

Discrete continuum method for investigation of linear and nonlinear dynamics of hybrid systems containing coupled multi deformable bodies was presented by Hedrih [5]. The systems of coupled rods, beams, strings, plates and membranes with discrete continuum massless layers as well as layers with translator and rotator inertia properties were investigated and phenomenological mappings in dynamics of these different real system were applied and identified.

Composing the proper mathematical model of mechanical system presents one of the most important steps in the description of the system dynamics and structural model formulation. Whereby the description of the system we suppose all the levels of exploring the kinetics characteristics of the systems and abilities of their improvement, control, regulation or some other usage of mechanical systems. On the other way said, mathematical modeling regard on the usage of mathematical language to present the behavior of practical systems. It plays the role of better understanding of systems features. Non-linearity appears both as an object's natural characteristic and the corresponding non-linearity of the systems of differential equations describing the system dynamics, which is a consequence of the choice of the coordinates of the system's description. Since the problem is to explore and in some possible way control non-linearity.

Theory is useful for presenting the general conclusions to the simple models while the computers are useful for obtaining the special conclusions for more complicated systems. However, in order to form a mathematical description of the complex system we are forced to introduce a number of assumptions, simplifications, neglect or possible measurement errors, and our structural model can have significant different dynamics from real physical models. To avoid this, it is useful to note the similarities in the physical phenomena and mathematical descriptions of the various systems and to take advantage in the general conclusions.

The paper by Hedrih and Simonovic [6] is a good example of this theory application and it presents mathematical models of several complex mechanical systems, introduces its analogies, and explains nonlinear phenomena of passing through resonant regions. Systems consist of coupled deformable bodies like plates, beams, or membranes that are connected through discrete continuum layer with nonlinear elastic and translator and rotator inertia properties. Visco-elastic non-linear layer, with properties of translation and rotation of added mass elements, was rheological modeled by continuously distributed elements of Kelvin-Voigt type with nonlinearity of third order with addition of rotatory elements. The formalism and results of these ideas will be summarised in the first section of this review.

The interest in the study of multi bodies systems, as new qualitative systems, dynamics has grown exponentially over the last few years because of the theoretical challenges involved in the investigation of such systems. Recent technological innovations have caused a considerable interest in the study of component and

hybrid dynamical processes of coupled rigid and deformable bodies (plates, beams and belts) (see Refs. [5–8] and [9]) denoted as hybrid systems, characterized by the interaction between subsystem dynamics, governed by coupled partial differential equations with boundary and initial conditions.

The study of transversal vibrations of multi bodies system with elastic, visco-elastic or creep connections is important for both theoretical and pragmatic reasons. The dynamic behavior of many important structures may be investigated from mathematical models of such a deformable bodies system. The models presented in this paper might be use in presentation of non-linear dynamics behavior for one number of real structures. For example, in civil engineering for roofs, floors, walls, in thermo and acoustics isolation systems of walls and floors constructions, orthotropic bridge decks or for building any structural application in which the traditional method of construction uses stiffened steel.

The sandwich constructions consist of two or more facing layers that are structurally bonded to a core made of material with small specific weight. This type of construction provides a structural system that acts as a crack arrest layer and that can join two dissimilar metals without welding or without setting up a galvanic cell and provides equivalent in plane and transverse stiffness and strength, reduces fatigue problems, minimizes stress concentrations, improves thermal and acoustical insulation, and provides vibration control. It is shown here that as a model of those structures it is possible to use a visco-elastically connected double deformable bodies system with non-linearity in elastic layer.

In many engineering systems with non-linearity, high frequency excitations are the sources of multi frequency resonant regimes appearance at high as well as at low frequency modes. That is obvious from many experimental research results and also theoretical results [10–11]. The interaction between amplitudes and phases of the different modes in the nonlinear systems with many degrees of freedom, as in the deformable body with infinite numbers frequency vibration in free and forced regimes, is observed theoretically in [12] by using averaging asymptotic methods Krilov-Bogoliyubov-Mitropolyskiy [13]. This knowledge has great practical importance.

In the monograph by Nayfeh [10] a coherent and unified treatment of analytical, computational, and experimental methods and concepts of modal nonlinear interactions is presented. These methods are used to explore and unfold in a unified manner the fascinating complexities in nonlinear dynamical systems.

Identifying, evaluating, and controlling dynamical integrity measures in nonlinear mechanical oscillators are topics for researchers, [8–14–17]. Energy transfer between coupled oscillators can be a measure of the dynamical integrity of hybrid systems as well as subsystems [7–16]. In the series of references, it is possible to find a different approach to obtain solutions of the nonlinear dynamics of real systems, as well to discover nonlinear phenomena or some properties of the system dynamics. There are many systems which consist of a nonlinear oscillator attached to a linear system, examples of which are nonlinear vibration absorbers, or nonlinear systems under test using shakers excited harmonically with a constant force.

List of the valuable research results in a related area of the objects of the author's research is large, but in this introduction the subjective choice was mentioned. The interested reader can find more references in the reference list of the doctoral thesis by Simonovic [9].

By using averaging and asymptotic methods for obtaining system of ordinary differential equations of amplitudes and phases in first approximations and expressions for energy of the excited modes depending on amplitudes, phases and frequencies of different nonlinear modes are obtained by Hedrih K. in [15–16] and by Hedrih K. and Simonović J. in [8]. By means of these asymptotic approximations, the energy analysis of mode interaction in the multi frequency free and forced vibration regimes of nonlinear elastic systems (beams, plates, and shells) excited by initial conditions was made, and a series of resonant jumps as well as energy transfer features were identified. Meaning that excitation was, by perturbation of equilibrium state of the double plate system at initial moment, defined by initial conditions for displacements and velocities of both plate middle surface points. In this review inside the section 2.3 the energies transfer in one eigen amplitude mode of oscillation of coupled system is analyzed. The new diagrams of time functions corresponding to specific eigen amplitude mod of oscillation are presented so that energy jumps and transfer between system elements and time modes can be analyzed according to established values of reduced energies that corresponds to system parts.

In the point of having mathematical model of modelled physical system we are able to analyze the influence of system's parameter changes on the behavior of system dynamics. It is easy to summarize influence of one ore two parameters. For instance, in the paper Simonovic (2015) [17] the influence of the mass of rolling elements has been investigated and amplitude/phase-frequency characteristic curves were compared for theree different values of rolling elements mass. The presence of rolling elements in the interconnected layer introduces the part of the dynamic coupling into mathematical model- the system of obtained PDE's. Also, this model with nonlinearity of the third order in the interconnected layer introduces the phenomenon of passing through resonant range and appearance of one or several resonant jumps in the amplitude–frequency and phase–frequency curves, as in the multi-nonlinear mode mutual interactions between amplitudes and phases of different nonlinear modes. Based on the presented numerical comparison it has been consequently concluded that dynamic coupling intensifies the phenomena of the resonant transition caused by the mutual interaction of the harmonics. The changes of one parameter we cross-correlated with the discrete and continuous changes of external excitation frequencies in the region of the resonant system frequencies for stationary and non-stationary resonant regimes. And since the numerical calculations were quite intense, and the number of obtained amplitude/phase frequencies characteristic curves were large it was necessary to find another method for analyzing a larger number of important parameters. Moreover, the presented analysis is suitable for the exploration of dynamics in the bounded regimes of oscillation. Consequently, we introduced the new method of mathematical model analysis for the investigation of the global dynamics named multi-parametric

analysis that allows us the simultaneous analysis of several parameter`s influences.

The proposed multi-parametric analysis has been exploited further, in the section 2.4, for identical synchronization (IS) appearance in the global dynamics of the same system of coupled deformable bodies with the layer of visco-elastic nonlinear elements with rolling properties.

The proposed multi-parametric analysis is applicable for research of IS of the systems with more degree of freedom and similar parameters of elastic, viscose, and dynamic coupling that can be simultaneously examined. The next model of interests presented in the section 3., is the model of chain lattice composed of the four chains with eleven material particles, as it was proposed by Simonovic [18]. Investigation of dynamics of chains of material particles in the systems with more than three degrees of freedom, even in the field of classical and linear chain forced dynamics, is important not only for mechanical signal processing, but also for electrical signal processing and signal filtering, for processing biodynamical signals in life systems (DNA double helix chains [19], biodynamical chain oscillators [20–21] and also for university teaching and integrations of scientific results in different scientific fields.

The acquired knowledge and skills of complex system dynamics analysis using mathematical analogies can be applied also in mechanobiology. Several years of research in that filed has been realized by two postdoc research period supported by European Union trough ERASMUS MUNDUS and Marie Skłodowska-Curie Actions (MSCA) frameworks. Two projects were realized: six-month post PhD research period, between December 2015 and June 2016, at Interdisciplinary Centre for Mathematical and Computational Modelling of Warsaw University on subject of Bone Tissue Advanced Modelling with Piezoelectricity; and two-year, 2017-2019, post PhD research period at Biomedical Engineering Department, School of Engineering, Cardiff University under the project "Mathematical Modelling of Bone Externally Excited Remodelling" (MMoBEER). Bone mechanobiology research how mechanical forces and loadings influences architecture and quality of bone tissue and it is important to establish proper mathematical model of this process. Although it is possible to mechanically stimulate bone and quantify the tissue-level changes that occur, it is still extremely challenging to simultaneously delineate the cellular and molecular mechanisms that give rise to these changes.

The following section 4. presents a nice application of the same concept of mathematical modelling and analogies application in bone mechanobiology. The scientific field that investigates how physical forces and changes in the mechanical properties of cells and tissues contribute to development, cell differentiation, physiology, and disease, in general, is mechanobiology. The governing system of differential equations that describe bone remodeling processes at the cellular level is the generalized Lotka-Volterra system or S-system with power low coefficients. The number of important parameters in such a system is large and it is possible to successfully use multi-parametric simultaneous analysis to reveal the desirable dynamics of the bone cells that ensure balanced resorption of old, damaged bone tissue and formation of new, healthy bone content. In the case of bone cellular modelling and structural mathematical modelling, both fields should benefit. Specifically, we gain more understanding of bone tissue development through developing more

mimetic models that can more realistically simulate real cell environment, which can be further used to predict treatment prognosis. Equally, the mathematical modelling improves as we develop new tools that deal with many different input and output parameters and variables and can be characterised as the mathematics of adaptive systems. Overall, joining theoretical and experimental approaches offers new paths for understanding, producing, simulating and predicting the features of a new generation of biomimetic trends (materials, experimental and measurement devices, mathematical predictions etc.).

All the examples in this review paper encompass and underline the variety, beauty, and power of mathematical formalism, modeling, and simulations that can be applied in disparate scientific research. Furthermore, the experiments with the mathematical calculation so-called in/silico experiments allow effective and efficient ways to explore reality.

2. Models of hybrid dynamical systems

In this chapter, we present a conceptual model of coupled multi-layered systems. Many important structures may be modeled from composite (multi-layered) structure and are necessary in many appliances. For example, in civil engineering for roofs, floors, walls, in thermo and acoustics isolation systems of walls, and floor constructions, orthotropic bridge decks or for building, any structural application in which the traditional method of construction is applied usage of stiffened steel. Also, it is applied in cars, planes and ships industry for sheaths of plain wings, for inner arrangement of plain, it is suitable for building maritime vessels or for building civil structures such as double hull oil tankers, bulk carriers, auto bodies, truck bodies or for railway vehicles. Furthermore, such construction may serve as a dynamic absorber system since it possesses several bodies some of which may play the role of the harvester of the energy of external excitation what we call natural absorption [22] or we can also detect nonlinear harvesting of energy due to the multi-mode nonlinear coupling in some of the nm mode of oscillations [7]. Our model of coupled structures contains several deformable bodies (plates, beam, belts, or membranes) connected with continually distributed layers of discrete rheological elements with various properties of elasticity, viscous, and nonlinear character, Fig.1.The first assumption in conceptual model is that he coupling layer is presented of infinite number od distrete rheological elements which ends moves coresponding to mid-plane (line) points transversal displacement of conected deformable bodies. The study of transversal vibrations of a double like multi body system with elastic, visco-elastic of creep connections is important for both theoretical and pragmatic reasons.

For standard rolling visco nonlinear elastic element, Figs. 1c) lighted on a way of the rheological models [23], we write the expressions for the velocity of translation for the centre of masse C, Fig 1. c), in the form: $\dot{w}_C = (\dot{w}_2 + \dot{w}_1)/2$, and for the angular velocity around center of mass in the form: $\omega_C = (\dot{w}_2 - \dot{w}_1)/2R$. The constitutive relations for forces on the ends of this element are in the following form:

$$F_{1(2)} = \pm\left(c + \frac{c_1}{4}\right)(w_2 - w_1) \pm b_1(\dot{w}_2 - \dot{w}_1) \pm \beta(w_2 - w_1)^3 - \frac{1}{4}m\left\langle(\ddot{w}_2 + \right.$$
$$\left. + \ddot{w}_1) \mp \frac{i_C^2}{R^2}(\ddot{w}_2 - \ddot{w}_1)\right\rangle \qquad (1)$$

where c and c_1 are stiffness of linear springs, $b_1$is coefficient of damping force, β stiffness of nonlinear springs, m is mass of disc, $i_C^2 = \boldsymbol{J_C}/m$ is the square of radius of axial mass inertia moment for the rolling element around central axis. If the rolling element is the disc then mass axial moment of inertia is $\boldsymbol{J_C} = R^2m/2$ and $i_C^2 = R^2/2$.

The governing equations of the double body-plate system [6–8–24], Figs. 1 a), b), e) and d), are formulated in terms of two unknowns: the transversal displacement $w_i(\wp, t)$, $i = 1,2$ in direction of the z axis, of the upper body-plate middle surface and of the lower body-plate middle surface, respectively. We present the interconnecting layer as a model of distributed discrete rheological rolling visco-elastic rolling elements with nonlinearity in the elastic part of the layer, as shown in Figure 1.c). Since that elements are continually distributed on plates surfaces, the generalized resulting forces (1) are also continually distributed onto middle plate surface points. Our assumptions for the plates are: they are thin with same contours and with equal type of the boundary conditions and they have small transversal displacements. The system of two coupled partial differential equations is derived using d'Alembert's principle of dynamic equilibrium in the following forms:

$$(1 + \tilde{a}_{\text{ii}})\frac{\partial^2 w_i(\wp,t)}{\partial t^2} + \tilde{a}_{12(i)}\frac{\partial^2 w_{i+1}}{\partial t^2} + c_{(i)}^4 \prod w_i(\wp, t) - 2\delta_{(i)}\left[\frac{\partial w_{i+1}(\wp,t)}{\partial t} - \frac{\partial w_i(\wp,t)}{\partial t}\right] -$$

$$-a_{(i)}^2[w_{i+1}(\wp, t) - w_i(\wp, t)] = \pm\varepsilon\beta_{(i)}[w_{i+1}(\wp, t) - w_i(\wp, t)]^3 + \tilde{q}_{(i)}(\wp, t)$$

$$\text{for } i = 1,2 \qquad (2)$$

where: $\hat{a}_{12} = m/4 - \boldsymbol{J_C}/4R^2 = m/8$; $\hat{a}_{\text{ii}} = m/4 + \boldsymbol{J_C}/4R^2 = 3m/8$; E = Young's modulus of bodies materials; μ_i= Poisson's coefficient; ρ_i=density of bodies material.

For circular plates we have: $\wp \equiv r, \varphi$ space middle surface coordinates; operator $\prod \equiv \Delta^2$. Reduction of coefficients are: $\tilde{a}_{\text{ii}} = \hat{a}_{\text{ii}}/\rho_i h_i$; $\tilde{a}_{12(i)} = \hat{a}_{12}/\rho_i h_i$; $a_{(i)}^2 = (c + c_1/4)/\rho_i h_i$; $D_i = E_i h_i^3/12(1 - \mu_i^2)$; flexural plate rigidity $c_{(i)}^4 = D_i/h_i$; $2\delta_i = b_1/\rho_i h_i$ and $\varepsilon\beta_{(i)} = \beta/\rho_i h_i$; for $i = 1,2$; h_i height of plates. The form ρ_i of the external loads on the bodies surfaces are given as $\tilde{q}_{(i)} = q_{(i)}(r, \varphi, t)/\rho_i h_i$.

For beams we have: $\wp \equiv z$ space line coordinate along neutral line of the beams; operator $\prod \equiv \partial^4/\partial z^4$; $\mathfrak{B}_i = E_i I_x$ flexural beam rigidity. Reductions of the coefficients are: $\tilde{a}_{\text{ii}} = \hat{a}_{\text{ii}}/\rho_i A_i$; $\tilde{a}_{12(i)} = \hat{a}_{12}/\rho_i A_i$; $c_{(i)}^2 = \sqrt{\mathfrak{B}_i/\rho_i A_i}$; $a_{(i)}^2 = c_e/\rho_i A_i$; $\varepsilon\beta_{(i)} = \beta/\rho_i A_i$; $2\delta_i = b/\rho_i A_i$; $\tilde{q}_{(i)} = q_{(i)}(z, t)/\rho_i A_i$.

For circular membranes we have: $\wp \equiv r, \varphi$ space surface coordinates; $\prod \equiv \Delta = \frac{\partial^2}{\partial r^2} + \frac{1}{r}\frac{\partial}{\partial r} + \frac{1}{r^2}\frac{\partial^2}{\partial \phi^2}$ is Laplacian operator. Reduction of the coefficients are: $\tilde{a}_{\text{ii}} = \hat{a}_{\text{ii}}/\rho_i$; $\tilde{a}_{12(i)} = \hat{a}_{12}/\rho_i$; $c_{(i)}^2 = \sigma_i/\rho_i$; $a_{(i)}^2 = c_e/\rho_i$; $\varepsilon\beta_{(i)} = \beta/\rho_i$; $2\delta_i = b/\rho_i$; $\tilde{q}_{(i)} = q_{(i)}(r, \varphi, t)/\rho_i$.

For belts we have: $\wp \equiv x$ line coordinate along neutral line lenght of belts; $\prod \equiv \Delta = \partial^2/\partial x^2$is Laplacian operator. Reduction coefficients are: $\tilde{a}_{\text{ii}} = \hat{a}_{\text{ii}}/\rho_i$; $\tilde{a}_{12(i)} = \hat{a}_{12}/\rho_i$; $c_{(i)}^2 = \sigma_i/\rho_i$; $a_{(i)}^2 = c_e/\rho_i$; $\varepsilon\beta_{(i)} = \beta/\rho_i$; $2\delta_i = b/\rho_i$; $\tilde{q}_{(i)} = q_{(i)}(x, t)/\rho_i$.

The sign $\pm$ on the right hand side of equations (2) corresponds to the soft (sign +) or hard (sign -) properties of the non-linear elastic layer.

The system of equation (2) represents a mathematical model of multi-body small transversal displacement and has the same form for different coupled bodies (plates, membranes, beams, or belts)only the coordinates of the mid plane (line) and the reduction parameters have different notation.

The asymptotic approximation of solution, in one eigen mod of oscillations, where number of eigen modes are $n, m = 1,2,3 \ldots \infty$ for plates or membranes, and $n = 1,2,3 \ldots \infty$ for beams or belts, for the system (1) is taken in the form of the eigen amplitude functions $W_{i(eign)}(\wp)$, satisfying the same boundary conditions and orthogonally conditions, multiplied with time coefficients in the form of unknown time functions $T_i(t)$, $i = 1,2$ and describing their time evolution (see Refs. [8–24–25]):

$$w_i(\wp, t) = W_{k(eign)}(\wp)\, T_{(i)k(eign)}(t) =$$
$$= W_{k(eign)}(\wp)\left[K^{(1)}_{2i,k(eign)} e^{-\hat{\delta}_{1(eign)}t} R_{1(eign)}(t)\cos\Phi_{1(eign)}(t) + \right.$$
$$\left. + K^{(2)}_{2i,k(eign)} e^{-\hat{\delta}_{2(eign)}t} R_{2(eign)}(t)\cos\Phi_{2(eign)}(t)\right] \qquad (3)$$

where: $K^{(s)}_{2i,k(eign)}$ co-factors of elements of second row and corresponding column of determinant corresponding to basic linear coupled system [9–24], for proper eigen characteristic number $-\hat{\delta}_{i(eign)}$ real parts of the appropriate pair of the roots of the characteristic equation, and unknown amplitudes $R_{i(eign)}(t)$ and phases $\Phi_{i(eign)}(t) = \Omega_{i(eign)}t + \varphi_{i(eign)}(t)$; $i = 1,2$; of unknown time functions $T_{(i)k(eign)}(t)$ which we are going to obtain by using the Krilov-Bogolyubov-Mitropolyskiy asymptotic method (see Refs. [12–13–26]). The proposed assumption for mathematical model is that nonlinearities are small and that interactions between eigen amplitude modes may be neglected, and we only consider interactions between time eigen modes in one eigen amplitude mode.

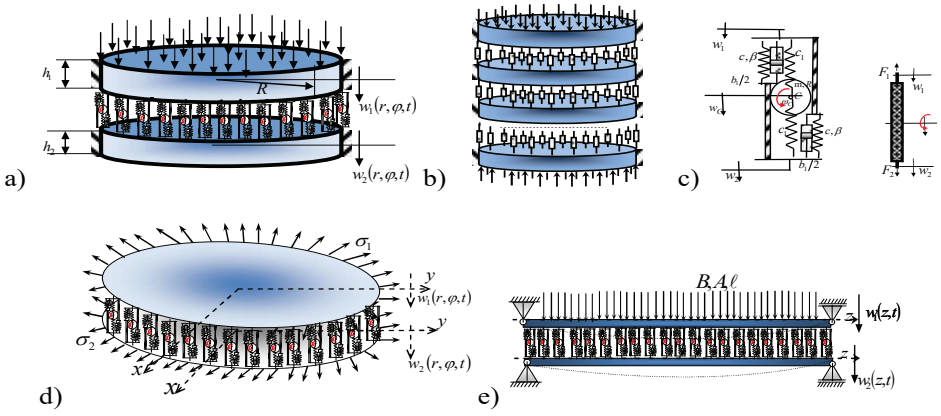

FIGURE 1. a) Double circular plate system; b) Multi plate system; c) the rheological model of rolling visco-elastic nonlinear discrete element; d) the rheological scheme of rolling visco-elastic nonlinear discrete element; f) double membrane system; g) double beam system.

After substituted this proposed asymptotic aproximation of solutions (3) in system of partial nonlinear differential equations (2), keeping in mind orthogonality conditions of body eigen amplitude functions $W_{i(eign)}(\wp)$ and $W_{j(eign)}(\wp)$, $i \neq j$, it turns out system of ordinary non-linear DE for eigen time functions $T_{(i)k(eign)}(t)$ of one eigen amplitude mode of considered class of the bodies transversal oscillations:

$$\begin{aligned}\ddot{T}_{(1)} + \kappa_1\ddot{T}_{(2)} - 2\tilde{\delta}_{(1)}\left(\dot{T}_{(2)} - \dot{T}_{(1)}\right) + \tilde{\omega}^2_{(1)}T_{(1)} - \tilde{a}^2_{(1)}T_{(2)} = \\ = \pm\varepsilon\tilde{\beta}_{(1)}\aleph\left(W_{eign}\right)\left[T_{(2)} - T_{(1)}\right]^3 + \tilde{f}_{(1)} \\ \ddot{T}_{(2)} + \kappa_2\ddot{T}_{(1)} + 2\tilde{\delta}_{(2)}\left(\dot{T}_{(2)} - \dot{T}_{(1)}\right) + \tilde{\omega}^2_{(2)}T_{(2)} - \tilde{a}^2_{(2)}T_{(1)} = \\ = \mp\varepsilon\tilde{\beta}_{(2)}\aleph\left(W_{eign}\right)\left[T_{(2)} - T_{(1)}\right]^3 - \tilde{f}_{(2)}\end{aligned} \quad (4)$$

where: $\tilde{\omega}^2_{(i)} = \omega^2_{(i)}/(1+\tilde{a}_{ii})$; $\aleph\left(W_{eign}\right) = \frac{\int_0^r\int_0^{2\pi} W^4_{(1)eign}\,rdr}{\int_0^r\int_0^{2\pi} W^2_{(1)eign}\,rdrd\phi}$ is coefficient of non-linearity influence of elastic layer, $f_{(i)}(t) = \frac{\int_0^r\int_0^{2\pi}\tilde{q}_i W_{(i)eign}\,rdrd\phi}{\int_0^r\int_0^{2\pi}\left[W_{(i)eign}\right]^2 rdrd\phi}$ are the known function of external forces and coefficients of reduction are: $\kappa_i = \tilde{a}_{12(i)}/(1+\tilde{a}_{ii})$, $\tilde{a}^2_{(i)} = a^2_{(i)}/(1+\tilde{a}_{ii})$, $2\tilde{\delta}_i = 2\delta_{(i)}/(1+\tilde{a}_{ii})$, $\tilde{\beta}_{(i)} = \beta_{(i)}/(1+\tilde{a}_{ii})$ and $\tilde{f}_{(i)nm} = f_{(i)nm}/(1+\tilde{a}_{ii})$. We intriduce denotation of $\omega^2_{(i)} = k^4_{(i)eign}c^4_{(i)} + a^2_{(i)}$, $i = 1,2$ for the square of eigen circular frequency of coupled body free linear vibrations, correspond to one eigen amplitude mode and corresponding time functions, obtained form system of ordinary differential equations (4) by omitting nonlinear terms and terms correspond to external exitation distributed along body middle surface in transversal directions.

The system of ordinary non-linear DE`s (4) is completely, pure mathematically, the same type for plate, beam, membrane or belt system of two coupled deformable bodies. The mathematical analogy is complete. By use phenomenological mapping a mathematical analogy between time functions $T_{(i)k(eign)}(t)$ in one eign amplitude mode of hybrid system dynamics is identified for corresponding multi beam, multi plate, multi membrane and multi belt system dynamics with layers of the same properties. Then, based on this phenomenological mapping and mathematical analogy, we present that solution for one type of the hybrid system dynamics is possible to use for the other to qualitative analysis linear or nonlinear phenomena appeared in dynamics.

It is considered that defined task satisfies all necessary conditions for applying asymptotic Krilov-Bogolyubov-Mitropolskiy method concerning small parameter of discrete continuum layer between bodies. We suppose that the functions of external excitation at one eigen mode of oscillations are the two-frequency process in the form: $\tilde{q}_{(i)eign}(t) = h_{01(eign)}\,cos\left[\Omega_{1(eign)}t\right] + h_{02(eign)}\,cos\left[\Omega_{2(eign)}t\right]$, and that external force frequencies $\Omega_{i(eign)}$ are in the range of two corresponding eigen linear damped coupled system frequencies $\Omega_{1(eign)} \approx \hat{p}_{1(eign)}$ and $\Omega_{2(eign)} \approx \hat{p}_{2(eign)}$

of the corresponding linear and free system to system (4) and that initial conditions of the double plate system permit appearance of the two-frequency like vibrations regimes of in one eigen amplitude mode of the system. $\hat{p}_{i(eign)}$ are frequencies of visco-elastic coupling obtained like imaginary parts of solution $\lambda_{i,j(eign)} = -\hat{\delta}_{i(eign)} \mp \mathrm{i}\hat{\mathrm{p}}_{i(eign)}$ for characteristic equations of system (4). More details and complete calculations could be find in Refs. [9–17, 25–27].

The observed case is that external distributed two-frequencies force acts at upper surfaces of upper body with frequencies near circular frequencies of coupling $\Omega_{i(eign)} \approx \hat{p}_{i(eign)}$, and that the lower body is free of excitation $\tilde{q}_{(2)eign}(t) = 0$. Then the first asymptotic averaged approximation of the system of differential equations for amplitudes $R_{i(eign)}(t)$ and difference of phases $\varphi_{i(eign)}(t)$ is obtained in the following general form, [6–8–9–24–26]:

$$\dot{a}_1(t) = -\delta_1 a_1(t) - \frac{\varepsilon P_1}{(\Omega_1 + \hat{p}_1)} cos\,\varphi_1 = \sigma_1(a_1(t), a_2(t), \varphi_1(t), \varphi_2(t), \Omega_{1s}, \Omega_{2s})$$

$$\dot{\varphi}_1(t) = (\hat{p}_1 - \Omega_1) - \frac{3}{8}\frac{\alpha_1}{\hat{p}_1} a_1^2(t) - \frac{1}{4}\frac{\beta_1}{\hat{p}_1} a_2^2(t) + \frac{\varepsilon P_1}{(\Omega_1 + \hat{p}_1) a_1(t)} sin\,\varphi_1 =$$
$$= \tau_1(a_1(t), a_2(t), \varphi_1(t), \varphi_2(t), \Omega_{1s}, \Omega_{2s})$$

$$\dot{a}_2(t) = -\delta_2 a_2(t) - \frac{\varepsilon P_2}{(\Omega_2 + \hat{p}_2)} cos\,\varphi_2 = \sigma_2(a_1(t), a_2(t), \varphi_1(t), \varphi_2(t), \Omega_{1s}, \Omega_{2s})$$

$$\dot{\varphi}_2(t) = (\hat{p}_2 - \Omega_2) - \frac{3}{8}\frac{\alpha_2}{\hat{p}_2} a_2^2(t) - \frac{1}{4}\frac{\beta_2}{\hat{p}_2} a_1^2(t) + \frac{\varepsilon P_2}{(\Omega_2 + \hat{p}_2) a_2(t)} sin\,\varphi_2 =$$
$$= \tau_2(a_1(t), a_2(t), \varphi_1(t), \varphi_2(t), \Omega_{1s}, \Omega_{2s}) \qquad (5)$$

where $a_i(t) = R_i(t) e^{-\hat{\delta}_i t}$ is the change of variables hence $\dot{a}_i(t) = \left(\dot{R}_i(t) - \hat{\delta}_i R_i(t)\right) e^{-\hat{\delta}_i t}$. The full forms of constants δ_i, α_i, β_i and P_i were presented in [[9–26] Simonovic (2012 a, b)]. Here it was underlined that these constants all rely on coefficients of coupling properties via cofactors $K_{2i}^{(s)}$, that δ_i depends of damping coefficients of visco-elastic layer $\tilde{\delta}_{(i)}$, εP_i depend of excited amplitudes, and α_i, β_i of non-linearity layer properties. Coefficients α_i, β_i are coefficients of eigen time mode mutual interactions.

It was observed the case when external distributed two-frequencies force in one eigen body amplitude mode acts at normal direction and along middle plain (line) of upper body with frequencies near eigen circular frequencies of corresponding coupled linearized plate systems $\Omega_i \approx \hat{p}_i$. In this case the lower body is free of load. This means that we were observed the passing thought main resonant states by discrete changing the values of the forced frequencies. By using the first asymptotic approximation of the amplitudes and phases of multi frequency particular solutions of eigen time functions of one eigen amplitude shape as well as of the non-linear system dynamics (5), we are in position to make analytical analysis of the stability of nonlinear modes in stationary regimes and to present results of theirs numerical solutions, for particular eigen time modes in one eigen amplitude mode of oscillations, $n, m = 1,2,3 \ldots \infty$ for plates (membranes) or $n = 1,2,3 \ldots \infty$ for beams (belts).

2.1. Multi-frequency analysis of the stationary resonant regimes of transversal vibrations of a double body system. For the analysis of the stationary resonant regimes of eigen time function mode oscillations correspond to one eigen amplitude function we were used analysis of amplitudes and phases for system of differential equations (5) in first approximation, obtained by Krilov-Bogolyubov-Mitropolyski method. For that reason, we equal the right-hand sides of differential equations (5) with null. Eliminating the phases ϕ_1 and ϕ_2 we obtained system of two non-linear algebraic equations by unknown amplitudes a_1 and a_2 (for detail see Refs. [9–26]). Also, with elimination of amplitudes a_1 and a_2, we obtained the algebraic equations for phases ϕ_1 and ϕ_2 in the case of two-frequency forced oscillations in stationary regime of one eigen (nm for plates or mode n for beams) mode of double bodies system oscillations. Solving these algebraic systems by numerical Newton-Kantorovic's method in computer program Mathematica, we obtained stationary amplitudes and phases curves of two-frequencies resonant regime of one eigen amplitude mode oscillations in double bodies system coupling with rolling visco-elastic nonlinear layer depending on frequencies of external excitation force in one amplitude mode and distributed along upper middle plate surface. If we fixed the value of on external excitation frequency of two possible, we obtained amlitude- and phase-frequency curves of stationary resonant vibration regime in the following forms:

1* for $\Omega_2 = const$ proper amplirude-frequency and phase-frequency curves of eigen time function modes in one amplitude mode are denoted by:
$a_1 = f_1(\Omega_1), a_2 = f_2(\Omega_1), \varphi_1 = f_3(\Omega_1)$ and $\varphi_2 = f_4(\Omega_1)$ and
2* for $\Omega_1 = const$ proper amplirude-frequency and phase-frequency curves of eigen time function modes in one amplitude mode are denoted by:
$a_1 = f_5(\Omega_2), a_2 = f_6(\Omega_2), \varphi_1 = f_7(\Omega_2)$ and $\varphi_2 = f_8(\Omega_2)$.

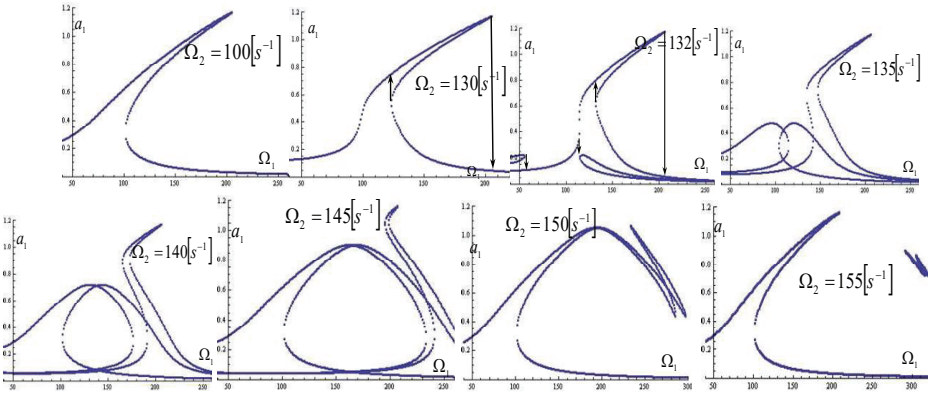

FIGURE 2. Amplitude-frequency characteristic curves for the amplitudes of the first time harmonics $a_{1nm} = f_1(\Omega_{1nm})$ of eigen time function modes in one amplitude mode on the different value of the excited frequency Ω_{1n} for the discrete value of the excited frequency $\Omega_{2nm} = const$ with noted corresponding one or more resonant jumps for $m = 240kg$. The arrows designate the directions of the resonant jumps.

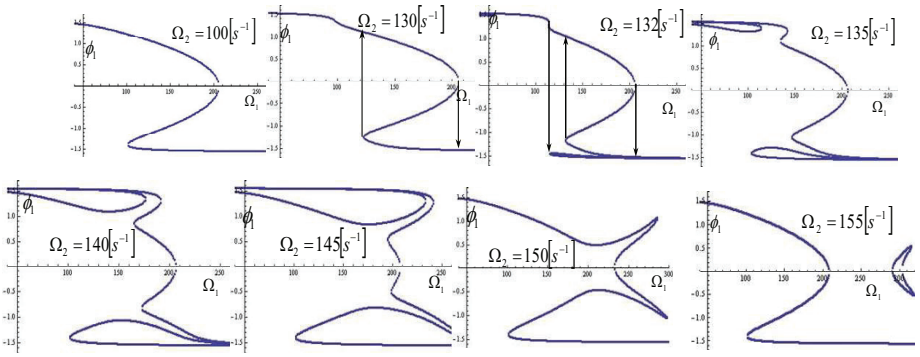

FIGURE 3. Phase -frequency characteristic curve for the phase of the first time harmonics $\phi_{1nm} = f_3(\Omega_{1nm})$ of eigen time function modes in one amplitude mode on the different value of the excited frequency Ω_{1nm}, for the discrete value of the excited frequency $\Omega_{2nm} = const$ with noted corresponding one or more resonant jumps for $m = 240\,kg$. The arrows designate the directions of the resonant jumps.

For any different discrete value of external force frequencies, we get characteristic diagram of that amplitide-frequency and proper phase-frequency curves of eigen time function modes in one amplitude modes. The Fig. 2 illustrates the series of that diagrams of eigen time function modes in one amplitude mode representing the passing through discrete stationary states alog resonant frequency intervals. We may follow the changes of amplitude and phase of eigen time function modes in one amplitude mode at that characteristic values of the frequencies of external force from the range of eigen frequencies of coupling in one eigen amplitude mode of proper linearized system oscillations.

The phenomena of the resonant transition for stationary regime are evident from diagrams. Those are the distinctive jumps of the amplitude and phase response in the vicinity of the resonant values $\Omega_i \approx \hat{p}_i$, appearance of the new stable and unstable branches causing the more value-system responses and the emergence of two stable solutions of the system in the area of those new branches, the mutual interaction of the time harmonics and the jumps of the system energies.

Characteristic for both series of the amplitude-frequency and phase-frequency curves of eigen time function modes in one amplitude modes is that more than one pair of the resonant jumps appears for two frequencies like non-linear stationary vibration regimes. Also, those jumps are followed by appearance of new instability branches, so there is more than one instability branches in the proper amplitude-frequency and phase-frequency curves. It is visible that in the listed discrete values of the external excitation frequency from the proper resonant intervals two pairs plus one or three pairs with one more resonant jump appear together with proper instable branch presented by dashed line in the listed figures.

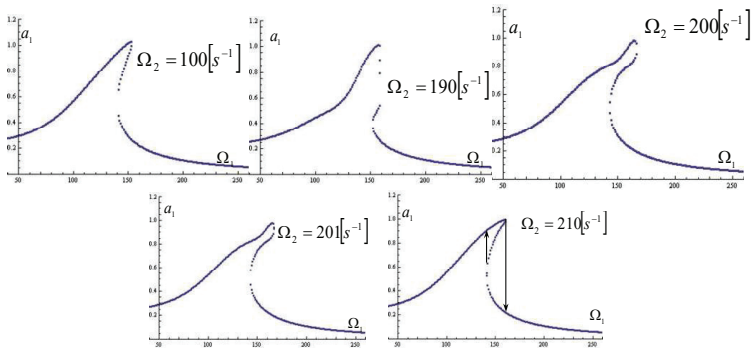

FIGURE 4. Amplitude-frequency characteristic curves for the amplitudes of the first time harmonics $a_1 = f_1(\Omega_1)$ of eigen time function modes in one amplitude mode for hard characteristics of interconnected layer and for the different discrete values of excited frequency $\Omega_2 = const$ with noted proper one or more resonant jumps, for $m = 0[kg]$. Arrows means directions of the resonant jumps.

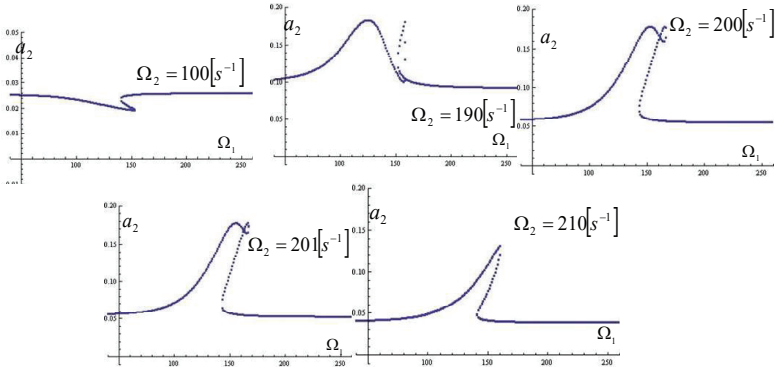

FIGURE 5. Amplitude -frequency characteristic curve for the amplitudes of the second time harmonics $a_{2nm} = f_2(\Omega_{1nm})$ of eigen time function modes in one amplitude mode on the different value of the excited frequency Ω_{1nm}, for the discrete value of the excited frequency $\Omega_{2nm} = const$ with noted corresponding one or more resonant jumps for $m = 0[kg]$.

Comparing the first and the last diagrams on the Figs. 4. and 5. we may conclude that the amplitude (same is for phase) responses of the first harmonic of eigen time function modes in one amplitude mode have small changes after transient regime, while the amplitude (phase) responses of the second harmonics have significant changes of the values and the shapes. Therefore, we conclude that the influence of the first harmonics on the second is greater in the resonant region of the frequencies Ω_{1nm} of external excitation, then the same influence in the resonant region of the frequencies Ω_{2nm} of external excitation.

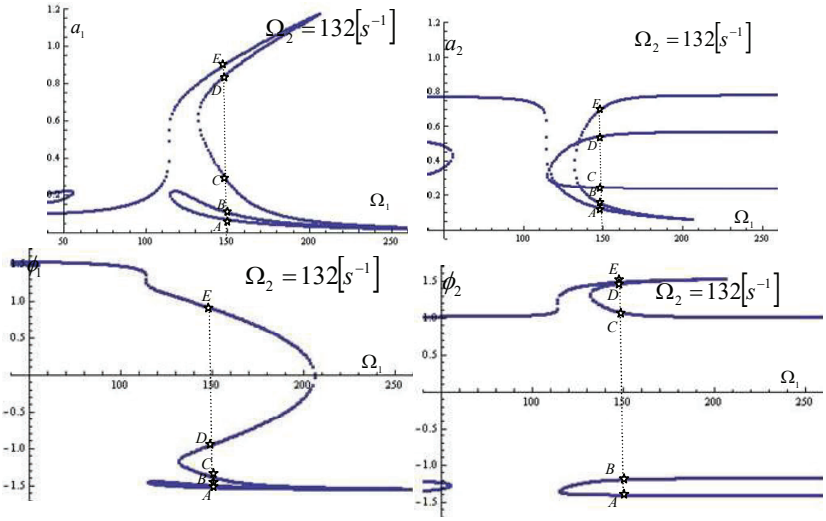

FIGURE 6. Frequency characteristic curves for the amplitude of the first time harmonic $a_1 = f_1(\Omega_1)$, for the amplitude of the second time harmonic $a_2 = f_2(\Omega_1)$, for the phase of the first time harmonic $\varphi_1 = f_3(\Omega_1)$ and for the phase of the second time harmonic $\varphi_2 = f_4(\Omega_1)$ of eigen time function modes in one amplitude mode on discrete value of excited frequency $\Omega_2 = 132[s^{-1}]$, with noted proper five stationary values on star points A, B, C, D and E.

For the case without rolling elements at the connected layer of the two plates, $m = 0\text{kg}$, on Figs. 4 and 5. for the select numerical particular values of the system parameters the interactions between two-time modes in one nm - th eigen amplitude shape mode of plates two frequency stationary like vibrations regime are presented. From the Fig. 4. it is noticable that amplitude-frequency curve of the first harmonics of eigen time function modes in one amplitude mode pass through resonant regime of the second frequency of external excitation without characteristic apearance of new branches, but the amplitude respons of the second harmonic has resonant jumps in the resonant range of the second frequency of external excitation $\Omega_{2nm} \in [185, 201]s^{-1}$ and after resonant transition undergo changes of values and shape. This also turned-out conclusion that first harmonic has more influence on the second then in the oposite case. Hence, the amplitude response in this case seems like in the case that there no nonlinearity we may turn out that influence of nonlinearity in the coupling layer is insignificant for such select of all other system parameters. The influence of the nonlinearity in the interconnected layer may be less or more present which depend on the parameters of the system. For example, by changing the value of the amplitude of the external excitations or coefficient of damping we may find the same phenomena of resonant transition, the resonant jumps and mutual modes interactions.

For obtaining data of stability or instability of the stationary amplitude and phase of eigen time function modes in one amplitude mode, it is necessary to use linearization

of the system of first approximation differential equations for two amplitudes and two phases (5) in each discrete stationary vibration state and to compose corresponding characteristic equation and to obtained corresponding roots. We could define local stability problem in a sense of Jacobian matrix of system (5). The eigen values of that matrix need to be known and explore consequently corresponding characteristic equation was composed. By using real parts of the roots of the evaluated characteristic equation it is possible to conclude whether the stationary two frequency like non-linear vibration regimes of eigen time function modes in one amplitude mode are stable or not. The values of these coefficients need to be valued for any value of Ω_{is} and determined values of a_{is} for $i = 1,2$ from the above diagrams and of ϕ_{is} from proper diagrams of phase-frequencies curves. For example, the noted star points A,B, C, or any else, on a diagrams at Fig. 6, has coordinate stationar values $(a_1; \phi_1; a_2; \phi_2; \Omega_1; \Omega_2)$. Than, the corresponding roots of the characteristic equation are obtained numerically, and for star point A we conclude that it is stable because the roots are all complex with negative real parts. All stationary valuses were numerically treated and if all real parts of the all roots of the characteristic equation are negative, then stationary resonant regime is stable. Since the solution is unstable if at least one of all roots has a positive real part. In the listed figures branches presented with dashed line corresponds to the expected unstable stationary vibration resonant regimes.

In the end of this section, we may discuss that obtained results for couple plates may be used for explanation of non-linear phenomenon in models of coupled beams, belts or membranes in connection with layer of same properties. All of them have same mathematical model in the time domain of their dynamics.

Using Petrovic's approach from [1–2], and comparing the results from the papers [28] with results in this paper, it is clear that there are analogies between non-linear phenomena in particular multi-frequency stationary resonant regimes of multi circular plate system non-linear dynamics and proper resonant forced regimes in chain system non-linear dynamics. Also, an analogy between non-linear phenomena in particular multi-frequency stationary resonant regimes of multi circular plate system non-linear dynamics and proper forced resonant regimes in multi-beam, membrane or belt system non-linear dynamics was here identified.

2.2. Controllability of the non-stationary resonant jumps. Strong interactions between time modes in the nm -th eigen amplitude shape mode of plate, appear only in the case that both values of both external excitation frequencies Ω_{1nm} and Ω_{2nm} are chosen simultaneously in the corresponding resonant frequency interval $\Omega_{inm} \approx \hat{p}_{inm}$. We introduce here the linear changes of the external frequencies in the proximity of the $\hat{p}_{inm}$ in the form: $\Omega_{inm} = \hat{p}_{inm} \pm \eta \cdot t$, where η is the rate of the linear changes.

The severity and speed of transitional jumps of this non-stationary regimes, Fig 7 a) and c), can be controlled by appropriate choice of the rate of external frequencies` changes. For instance, up to down jump, blue arrow line on the Fig.7 b), has several characteristics jumps after the first one that faster reaches main cure as the external frequency has slower changes, blue line on the Fig. c) for $\Omega_{1nm} = 170 + 5 \cdot t$. For faster transition changes of external frequencies, lines red and green on the Fig.7 c) for $\Omega_{1nm} = 170 + 10 \cdot t$ and $\Omega_{1nm} = 170 + 20 \cdot t$, subsequent jumps are more

numbered but less sharp. Faster transition passage in the resonant intervals is more dangerous with sharper sudden jumps in both directions: up to down, Fig.7 c), likewise bottom to top, Fig 7 a).

These considerations give the conclusion that the transition unexpected system jumps could be controlled by appropriate choice of the rate of the external frequencies` changes.

2.3. Analysis of energy transfer between nonlinear mode of oscillation in the *nm*-th eigen amplitude shape mode of coupled deformable bodies.

Following the established ideas and clarified proofs in the extensive work of Hedrih K. [16] and Simonovic [7–9] it is possible to analyze energy stream between coupled bodies in evry nm-th eigen amplitude shape mode where it is obvious that, due to the nonelinearity and coupling layer presence and time mode mutual interaction, exist the energy transfer between time modes and also energy mutation in one mode caused by changes in other mode. The energy flow between potential and kinetic energy present in conservative system with constant total energy cannot be accepted in this system not only due to the dissipation energy of damping elements properties but also due to nonlinearity and external sources of periodic forces.

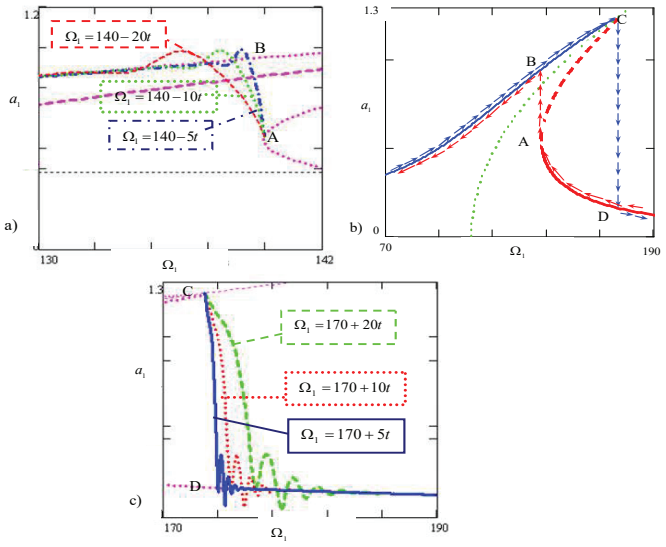

FIGURE 7. Amplitude-frequency characteristic curves for the amplitudes of the first time harmonics $a_{1nm} = f_1(\Omega_{1n})$ for the discrete value of the excited frequency $\Omega_{2nm} = const$. Three different rates of the resonant passage in both directions: a) Bottom to top jumps (point A to B on the middle diagram b)) during the decreasing of external excitation frequency $\Omega_{1nm} = 140 - 5 \cdot t$, $\Omega_{1nm} = 140 - 10 \cdot t$ and $\Omega_{1nm} = 140 - 20 \cdot t$ and c) Up to down jumps (point C to D on the middle diagram b)) during the increasing of external excitation frequency $\Omega_{1nm} = 170 + 5 \cdot t$, $\Omega_{1nm} = 170 + 10 \cdot t$ and $\Omega_{1nm} = 170 + 20t$. b) Nonlinear amplitude jumps occurring at the end points of non-stable branch (AC) of amplitude-frequency curve.

Energy harvesting of external source in coupled nonlinear systems depends on multimode coupling and nonlinear interaction of mode that can be analyzed using the ideas of reduced values of energy parts that belong to system elements. In that sense we distinguish the following parts of reduced values of energies in one nm -th eigen amplitude shape mode, where orthogonality conditions apply in form $v_{(i)nm}(r,\varphi)=\iint_A\left[W_{(i)nm}(r,\varphi)\right]^2 rdrd\varphi,\ i=1,2$, of oscillation that belong to first and second coupled element:

A.1* Kinetic energy of coupled bodies $i=1,2$:

$$\tilde{\tilde{E}}_{knm(i)}=\frac{1}{2}\rho_i h_i\left(\dot{T}_{(i)nm}(t)\right)^2=\frac{E_{k(i)nm}}{v_{(i)nm}} \tag{6a}$$

and part of kinetic energy caried by bodies originating from rolling parts of coupling layer:

$$\tilde{E}_{k(i)nm(1,2)layer}=\frac{\hat{a}_{ii}}{2}\left(\dot{T}_{(i)nm}(t)\right)^2=\frac{E_{k(i)nm(1,2)layer}}{v_{(i)nm}} \tag{6b}$$

A.2* Kinetic energy of interaction between bodies due to the rolling elements in interconnected layer:

$$\tilde{E}_{knm(1,2)layer,int}=\frac{\hat{a}_{12(1)}\hat{a}_{12(2)}\dot{T}_{(1)nm}(t)\dot{T}_{(2)nm}(t)}{2}=\frac{E_{knm(1,2)layer,int}}{v_{(i)nm}} \tag{6c}$$

B.1* Potential energy of bodies together with potential energy of visco-elastic layer that belongs to every body:

$$\tilde{\tilde{E}}_{pnm(i)}=\frac{1}{2}\rho_i h_i\omega_{(i)nm}^2\left(T_{(i)nm}(t)\right)^2=\frac{E_{p(i)nm}}{v_{(i)nm}} \tag{6d}$$

B.2* Potential energy of interaction caused by visco-elastic properties of layer:

$$\tilde{\tilde{E}}_{pnm(1,2)}=-\left(\rho_1 h_1 a_{(1)}^2+\rho_2 h_2 a_{(2)}^2\right)T_{(1)nm}(t)T_{(2)nm}(t)=\frac{E_{pnm(1,2)}}{v_{(i)nm}} \tag{6e}$$

By analysing potential energy of system, we can separate the following parts:

B.3 * reduced potential energy of every body without parts belonging to potential energies of elastic parts of layer:

$$\tilde{\tilde{\boldsymbol{E}}}_{pnm(i)}=\frac{1}{2}\rho_i h_i\omega_{0n}^2\ \left(T_{(i)nm}(t)\right)^2=\frac{\boldsymbol{E}_{pnm(i)}}{v_{(i)nm}} \tag{6f}$$

B.4* Reduced potential energy of elastic layer:

$$\tilde{\tilde{\mathbf{E}}}_{pnm(1,2)layer}=\frac{1}{2}c\left[T_{(2)nm}(t)-T_{(1)nm}(t)\right]^2=\frac{\mathbf{E}_{pnm(1,2)layer}}{v_{(i)nm}} \tag{6g}$$

where eigen frequencies of bodies are: $\omega_{(i)nm}^2=c_{(i)}^4k_{(i)nm}^4+a_{(i)}^2=\omega_{0nm}^2+a_{(i)}^2$.

At this manner we separated total potential energy to the parts belong to potential energy of bodies on the Winkler-type ground and potential energy of coupling layer corresponding to the bodies and a part corresponds to the interaction between bodies that depends only on rigidity of elastic layer and time functions of both bodies.

C.1* Rayleigh function of dissipation-the reduced part from visco-elastic layar corresponding to the bodies:

$$\tilde{\tilde{\Phi}}_{nm(1,2)layer(i)} = \delta_{(i)}\rho_i h_i\left(\dot{T}_{(i)nm}\right)^2 = \frac{\Phi_{nm(1,2)layer(i)}}{v_{(i)nm}} \tag{6h}$$

C.2* Rayleigh function of dissipation- only from interaction between bodies caused by the visco-elastic layer:

$$\tilde{\tilde{\Phi}}_{nm(1,2)layer} = -\left(\delta_{(1)}\rho_1 h_1 + \delta_{(2)}\rho_2 h_2\right)\dot{T}_{(1)nm}\dot{T}_{(2)nm} = \frac{\Phi_{nm(1,2)layer}}{v_{(i)nm}} \tag{6i}$$

Since the form of time functions corresponding to the nm -th eigen amplitude shape mode is presented by the form (3) we can only add the first time derivatives in the forms:

$$\begin{aligned}\dot{T}_{(1)nm}(t) = {} & K^{(1)}_{21nm}\dot{a}_{1n}\ (t)\cos\Phi_{1nm}(t) \\ & - K^{(1)}_{21nm}a_{1n}\ (t)(\Omega_{1nm} + \dot{\varphi}_{1n}\ )\sin\Phi_{1nm}(t) \\ & + K^{(2)}_{21nm}\dot{a}_{2n}\ (t)\cos\Phi_{2nm}(t) \\ & - K^{(2)}_{21nm}a_{2n}\ (t)(\Omega_{2nm} + \dot{\varphi}_{2nm})\sin\Phi_{2nm}(t)\end{aligned}$$

$$\begin{aligned}\dot{T}_{(2)nm}(t) = {} & K^{(1)}_{22nm}\dot{a}_{1nm}(t)\cos\Phi_{1nm}(t) \\ & - K^{(1)}_{22nm}a_{1nm}(t)(\Omega_{1nm} + +\dot{\varphi}_{1nm})\sin\Phi_{1nm}(t) \\ & + K^{(2)}_{22nm}\dot{a}_{2n}\ (t)\cos\Phi_{2nm}(t) \\ & - K^{(2)}_{22nm}a_{2nm}(t)(\Omega_{2nm} + +\dot{\varphi}_{2nm})\sin\Phi_{2n}\ (t)\end{aligned}$$

having in mind the first asymptotic solutions of amplitude and phase of both time harmonics given by the expressions (5) it is obvious that any changes and features that these solutions behave affect the changes of time harmonics of both functions. All the characteristic phenomena of the system dynamics, such as amplitude and phase jumps, stable and unstable new born branches of back-bone curve during transition stationary changes in resonant domain of both two frequencies oscillatory regimes of external loading, nonstationary amplitude jumps in both directions of increasing and decreasing of external frequencies in transition regimes, mutual interaction of both time harmonics in these regimes, determines the behavior of the energies parts of the system. All the reduced values of the energies relay on the shape of time harmonics and/or their time derivatives, expressions (6a-i), and their changes determines changes and energies jumps and transfers between system parts.

Time function of the first eigen shape of oscillation, whose shapes in the resonant region of the second excitation frequency are presented in Fig. 10, compounds of two mutually connected time harmonics. The time

harmonics vary shapes by passage through resonant regions and the curves are presented for both harmonics at the Figs. 8 and 9. We can conclude that the first time harmonic has a bigger influence since the shape of the time function, Fig. 10, is more similar to the shape of the first nonlinear time-harmonic, Fig. 8, than to the shape of the second time harmonics, Fig. 9. Since the reduced value of the potential energy of the first body, Eq. (6f), is directly proportional to the value of the time function corresponding to the particular eigen shape of oscillation we can suggest that the shape of that energy is similar to the shapes presented in Fig. 10, where we notice numerous jumps of energy by passage trough this resonant region. The further analysis can be performed also for first derivatives of time harmonics and functions which gives shapes similar to shapes of reduced values of kinetic energies Eqs. (6a, b) and energies of dissipation Eqs. (6h, i). Considering the length of this review paper the curves of that time derivatives were not presented but of course, it is not hard to get them once we have established mathematical models, Eqs. (4) and its first asimptotic aproximations for amplitude and phase Eqs. (5) of proposed solutions Eqs. (3). On the basis of the complete presentation, we could get the impression of the energy transfer in this complex dynamical behavior of hybrid structures of coupled deformable bodies.

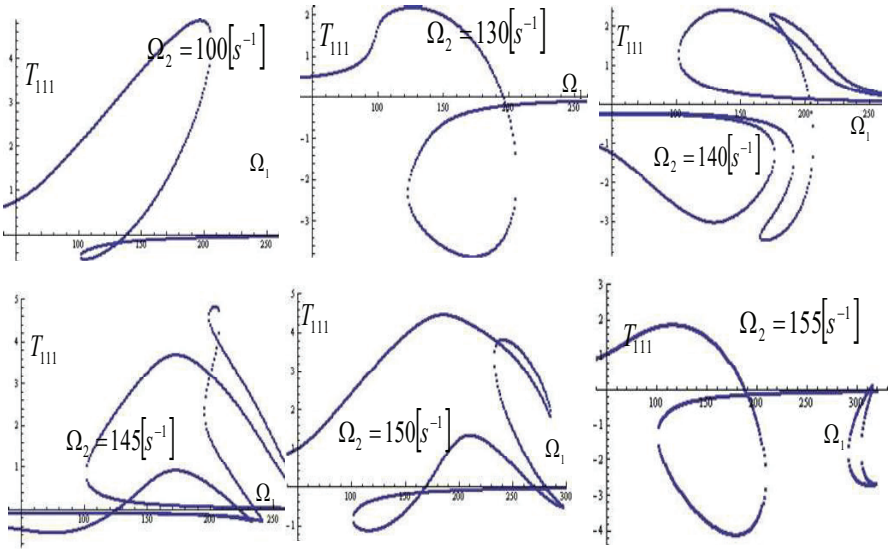

FIGURE 8. Time function of the first harmonics
$T_{111_1}(\Omega_1, \Omega_2) = 4.437 \cdot a_1(\Omega_1, \Omega_2 = const)\, cos[\Omega_2 \cdot t + \varphi_1(\Omega_1, \Omega_2 = const)]$ depending on frequency Ω_{1nm} and for discreet values of the second excitation frequency $\Omega_{2nm} = 100s^{-1}, 130s^{-1}, 140s^{-1}, 145s^{-1}, 150s^{-1}, 155s^{-1}, m = 240[kg]$

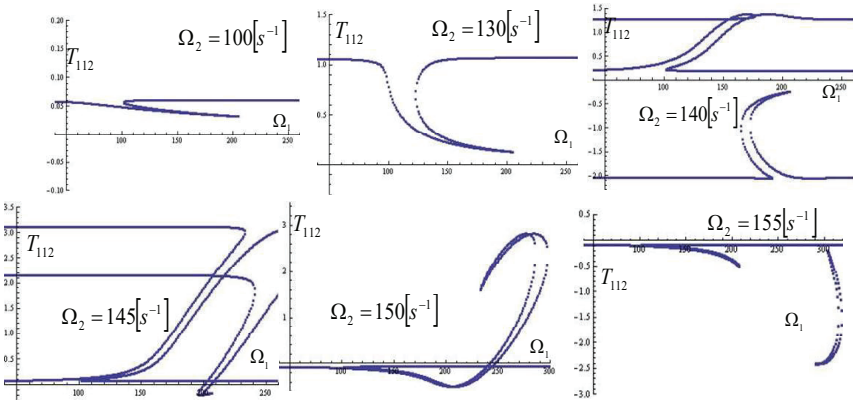

FIGURE 9. Time function of the second harmonics
$T_{111_2}(\Omega_1, \Omega_2) = 2.397 \cdot a_2(\Omega_1, \Omega_2 = const)\, cos[\Omega_2 \cdot t + \varphi_1(\Omega_1, \Omega_2 = const)]$
depending on frequency Ω_{1nm} and for discreet values of the second excitation frequency $\Omega_{2nm} = 100s^{-1}, 130s^{-1}, 140s^{-1}, 145s^{-1}, 150s^{-1}, 155s^{-1}$, $m = 240[kg]$

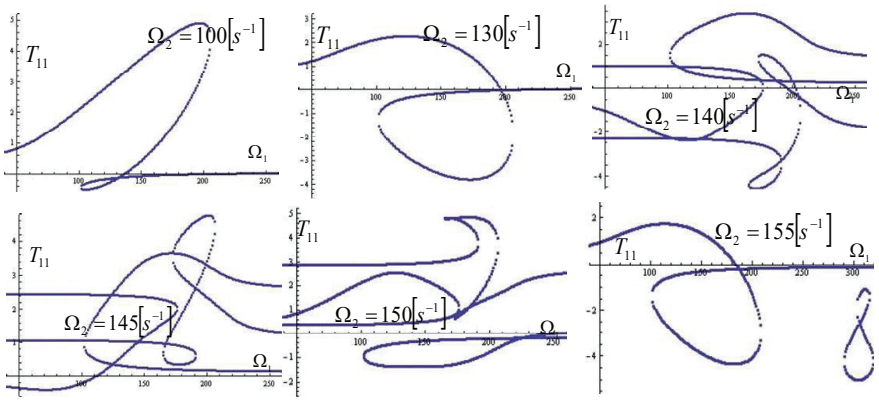

FIGURE 10. Time function of the first eigen shape of ocillation
$T_{111}(\Omega_1, \Omega_2) = 4.437 \cdot a_1(\Omega_1, \Omega_2 = const)\, cos[\Omega_2 \cdot t + \varphi_1(\Omega_1, \Omega_2 = const)] +$
$+2.397 \cdot a_2(\Omega_1, \Omega_2 = const)\, cos[\Omega_2 \cdot t + \varphi_1(\Omega_1, \Omega_2 = const)]$ depending on frequency Ω_{1nm} and for discreet values of the second excitation frequency $\Omega_{2nm} = 100s^{-1}, 130s^{-1}, 140s^{-1}, 145s^{-1}, 150s^{-1}, 155s^{-1}, m = 240[kg]$

2.4. Multi-parametric analysis of Identical Synchronization (IS) in double plate systems with layer of rolling visco-elastic non-linear elements. The first asymptotic solutions for amplitude and phase changes (5) stand for transition changes in resonant regimes for a small time interval thus

we can use them for analysis of local behaviour of system dynamics. However, the global behaviour of system dynamics play important role in many application and real consumption of construction. For instance, identical synchronization (IS) can only be examined on long time scales and shows global dynamics possibilities of adjustment of system parts with an external signal. Once established IS can be changed by parameter alteration and there exists parameter regions that ensure conditions for IS even though the initial conditions of coupled dynamics can be different. To explore these parameters basin that gives IS it is suitable to use a multi-parametric analysis of the system based on the established mathematical model (4).

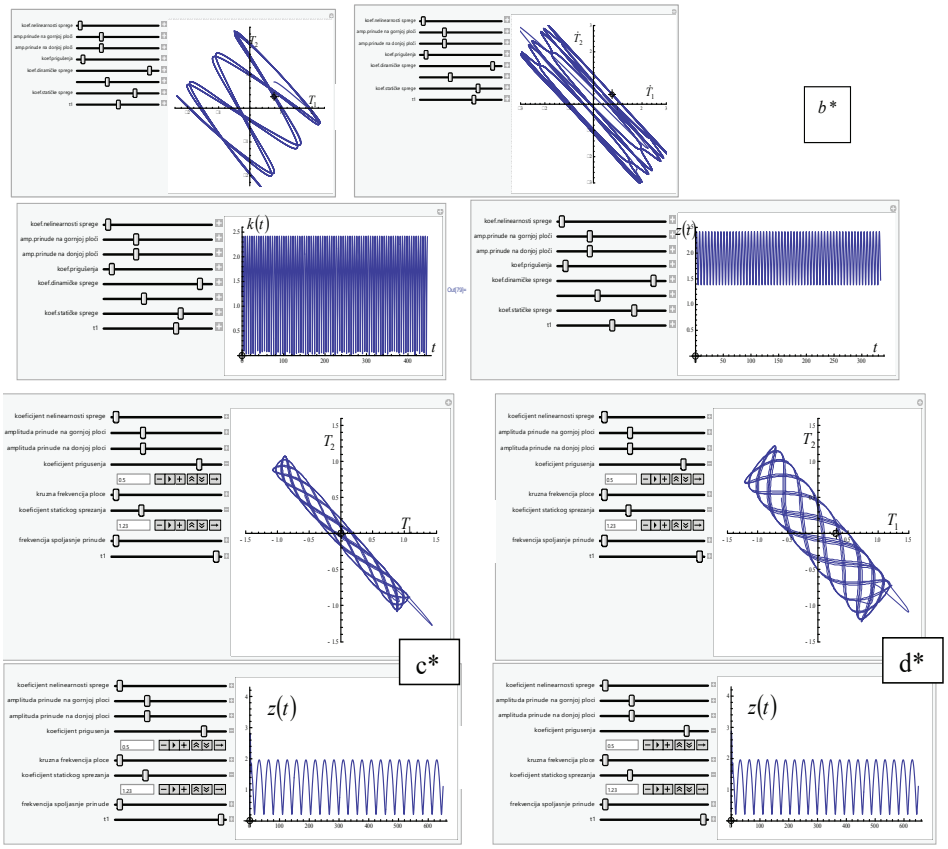

FIGURE 11. The characteristic synchronization attractor in a time domain of plates forced oscillations with the same external forces amplitudes and proper diagrams of synchronization error $z(t)$ and function $k(t)$ for : $\kappa_1 = \kappa_2 = 0.835$ and $\tilde{a}^2_{(i)} = 0.0468$ and different initial conditions : a* a* $T_1(0) = T_2(0) = 0.4; \dot{T}_1(0) = \dot{T}_2(0) = 0.4$ and b* $T_1(0) = \dot{T}_1(0) = 0.8; T_2(0) = \dot{T}_2(0) = 0.4$ *and* c* different parameter values $a^2_{(i)} = 1.23$, $\delta_{(1)} = \delta_{(2)} = 0.25$ and $\kappa_1 = \kappa_2 = 0$, and initial conditions: $T_1(t) = 0; T_2(t) = 0.2; \dot{T}_1(t) = \dot{T}_2(t) = 0;$ d* same parameters as for c* and different initial conditions $T_1(t) = 0.3; T_2(t) = 0.2; \dot{T}_1(t) = \dot{T}_2(t) = 0$

Possibilities for IS differ of the nature of coupling elements as it was verified in [29]. In our example the coupling element is rather complicate with the dynamic, static, nonlinear and damping properties, Fig. 1.d*. Such kind of element should be the represent of material properties such are nonlinear elasticity, viscosity and rolling of connected material.

This example with forced plates, with external forces in opposite direction, coupled with layer of rolling visco-elastic nonlinear elements presented with coupled time domain DE (4) for one nm -mode of oscillation may be explored in a sense of synchronization possibilities by changing the parameters of coupling. Here it is interesting phenomena that we expect resynchronization i.e., the situation when synchronization diagram is in the second and fourth quadrant because of opposite direction of forces. The value of resynchronization error is:

$$z_a(t) = \sqrt{\frac{1}{\varpi^2}(-T_1 - T_2)^2 + \left(-\dot{T}_1 - \dot{T}_2\right)^2} \tag{7}$$

The shape of attractors resynchronization can be changed by changing the coefficients of static and dynamic coupling. The form of the characteristic attractor do not changed by choosing the different initial values for proper relations of dynamic and static properties of coupling but its dimensions changed, Fig. 11.a* and b*. Synchronization error and value $k_a(t) = |-T_1 - T_2|$ are quasi periodic functions with greater absolute values for bigger synchronization attractor and changed its phase modulation by changing initial values. The alteration and changes of parameters` value in the system (4) can be simultaneously explored in Mathematica program by defining as many parameters as necessary and them simply by scrolling the left-hand side buttons, Fig. 11. which corresponds to parameter values we can visualize the synchronization diagram changes in time.

By increasing the coefficient of damping the dimensoins of synchronization attractor decrease. Sufficiently large value of damping coefficient might introduce the synchronization instead resynchronization. Since, dimensoins of resynchronization attractor in a second and fourth quadrant decrease by increasing the coefficient of damping. So its dimension in a diagonal direction of first and third quadrant increase and we have synchronization attractor and presents error of synchronization (6) with time function $T_{(i)}(t)$ as a variable.

We have here transition from attraction to repulsion in a time domain of plates dynamics at a critical coupling strength. This might be clearer by comparing the diagrams from the Figs. 11. b* and 12. which are done for all same values of parameters and initial conditions but for different value of damping coefficient of coupling.

The scroll labels in the Figs. 10 and 11 have the meaning of coefficient values which could be easy changed, and the diagram of synchronization gives the information of synchronization possibilities. These ideas of using the possibilities of the Mathematica program for easy and fast checking of synchronization phenomena may have the great practical importance.

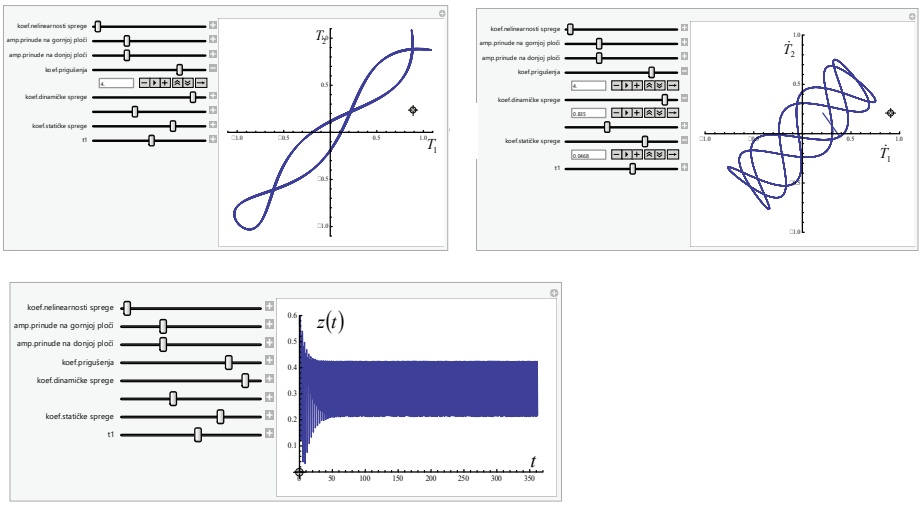

FIGURE 12. Diagrams of time function $T_1 - T_2$, $\dot{T}_1 - \dot{T}_2$ and synchronization error function of forced plate system coupled with layer of rolling visco-elastic nonlinear elements. With dynamic and static coefficients of coupling: $\kappa_1 = \kappa_2 = 0.835$ and $\tilde{a}^2_{(i)} = 0.0468$., whereby the coefficient of nonlinear coupling has value $\tilde{\boldsymbol{\beta}}_{\boldsymbol{i}} = \mathbf{0.1}$, and damping coefficient is $2\tilde{\delta}_{(i)} = 4$ with initial conditions $T_1(0) = \dot{T}_1(0) = 0.8$; $T_2(0) = \dot{T}_2(0) = 0.4$

3. Models of lattice of non-linear chains of material particles

The proposed multi-parametric analysis, in the previous section applied to global dynamics identical synchronization of coupled bodies, is applicable for research of IS of the systems with more degree of freedom and similar parameters of elastic, viscose, and dynamic coupling that can be simultaneously examined. The next model of interests is the model of chain lattice composed of the four chains with eleven material particles, as it was proposed by Simonovic [18]. The chains are orthogonally crossed on the third and the ninth particles noted as the knots, so there is two horizontal and two vertical chains, Fig. 13. Thus, we have forty-four coupled equations of motions in the form:

$$m_{(u)}\ddot{u}_{ij} = c_{(u)}\left(u_{i+1.j} - 2u_{i.j} + u_{i-1.j}\right) + \tilde{c}_{(u)}\left(u_{i+1.j} - u_{i.j}\right)^3 - \tilde{c}_{(u)}\left(u_{i.j} - u_{i-1.j}\right)^3 + \\ + b_{(u)}\left(\dot{u}_{i+1.j} - 2\dot{u}_{i.j} + \dot{u}_{i-1.j}\right) + h_{Ui.j}\cos\left(\Omega_{ij}t + \alpha_{ij}\right)$$

$$\text{for} \quad i = 1..4, j = 1....11 \qquad (8)$$

Investigation of dynamics of chains of material particles in the systems with more than three degrees of freedom, even in the field of classical and linear chain forced dynamics, is important not only for mechanical signal processing, but also for electrical signal processing and signal filtering, for processing biodynamical signals

in life systems (DNA double helix chains [19], biodynamical chain oscillators [20–21]) and also for university teaching and integrations of scientific results in different scientific fields.

To solve system of coupled differential equations (8) we were forced to use numerical simulation to obtain conclusions about possibilities of knots IS. We assume that horizontal and vertical directions of motion are independent, so for a general trajectory of knots motions we sum of the solutions from independent directions. For possible identical synchronization of vertical knots we are looking for the equality $x_3(t) + y_3(t) = u_3(t) + y_9(t)$ or $x_9(t) + v_3(t) = u_9(t) + v_9(t)$ and for possible synchronization of horizontal knots $x_3(t) + y_3(t) = x_9(t) + v_3(t)$ or $u_3(t) + y_9(t) = u_9(t) + v_9(t)$ and similar for the opposite combinations of knots. We also can provide different direction and position of the external excitation by changing the angle of attack on the particles α_{ij} and also position of the forces itself, Fig. 13.

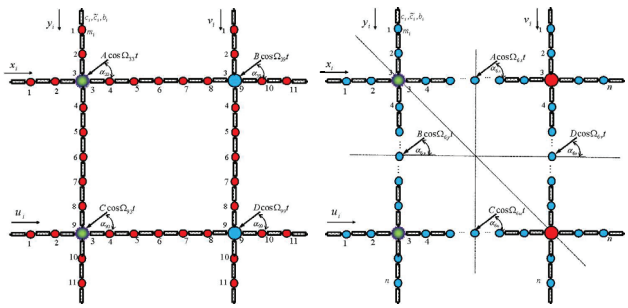

FIGURE 13. Crossed chains with knot external excitation or with excitation in the middle of the chains

In the left part of the Fig. 13 all four knots are attacked with external forces and we changed amplitudes and angles of attack like as values of coupling coefficients to synchronize them. The right part of the Fig. 13 presents possible attacks on the middles of the vertical chains, which perhaps give possibility of the diagonal symmetry of the lattice with synchrony of the opposite knots.

We were looking for the diagonal $x_3(t) + y_3(t) = u_3(t) + y_9(t)$ for exploration of synchronization of nodes on first vertical chain (nodes 33 and 39). That was naturally possible in the completely symmetric lattice when external excitations perform for notes in the same manner. The nodes adjust the resulting movements, and the synchronization attractor is visible after transition changes, Fig. 14. But for the value of the coefficient of linear coupling larger than 2.08, Fig. 14, middle part, the diagonal attractor is possible; the identical synchronisation is reached after some initial period of time called synchronization time. By increasing the damping coefficient, the synchronisation time is smaller, the nodes are synchronised faster when the coupling is with greater damping coefficient. The following observation was IS of the opposite nodes 33 and 99, Fig. 15, for the same case of symmetrically

excited lattice. Synchronization of opposite nodes is less possible even though for larger values of coefficient of linear coupling, upper part of the Fig. 15. But only increasing the damping coefficient the IS emerges even for the less values of the coupling strength, lower part of Fig. 15 the diagonal of synchronisation is visible.

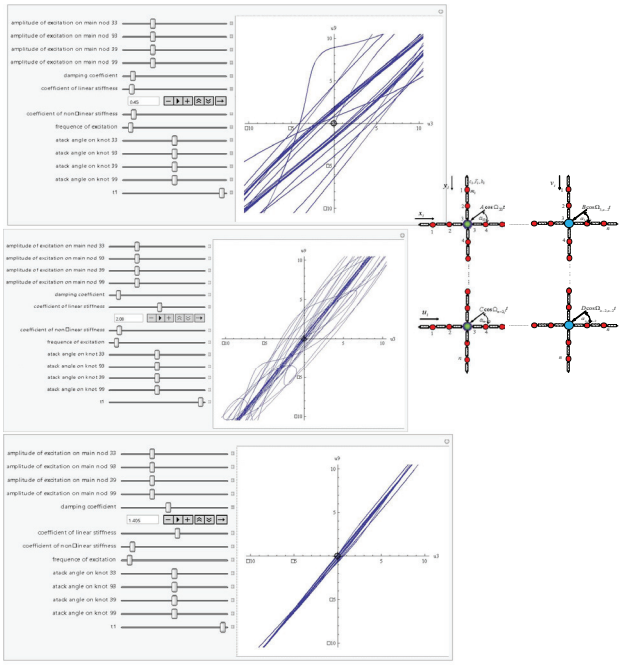

FIGURE 14. Synchronization attractors for knots from left vertical chain. External excitation acts on all four nodes.

When lattice is not attacked symmetrically, for example when external excitation acts on nodes 33, 39 and 99, the IS is impossible, Fig. 16. But after transition changes the different forms of phase synchronization are possible and the synchronization attractor is visible.

The upper part of Fig. 16 presents phase synchronisation 3:1, and the lower part phase synchronisation 1:1. By increasing coefficient of linear coupling the possibilities of synchronization increase after transition process, middle part of the Fig. 16. Increasing the frequency of excitations, the phase locking 1:1 of nodes gets better possibilities.

For the case when external excitations act on the middle of the chains like it was presented on the right part of Fig. 13, we have interesting phenomena of initial synchronization of knots, the diagonal line that is visible in the beginning of the motion, Fig. 17 upper part. In initial periods nodes are synchronize but after some period lost IS, it is necessary that signal from external excitation from the middle of chain reaches to the node after some initial period and to disturb the synchrony. Increasing the time period, we lost synchrony, Fig. 17 lower part.

By increasing coefficient of linear coupling the period of time in a synchrony of nodes is longer, Fig. 18, we can notice that the period of time is the same as on the lower part of Fig. 17, but there is diagonal line representing IS because of the greater value of the coefficient of the linear coupling.

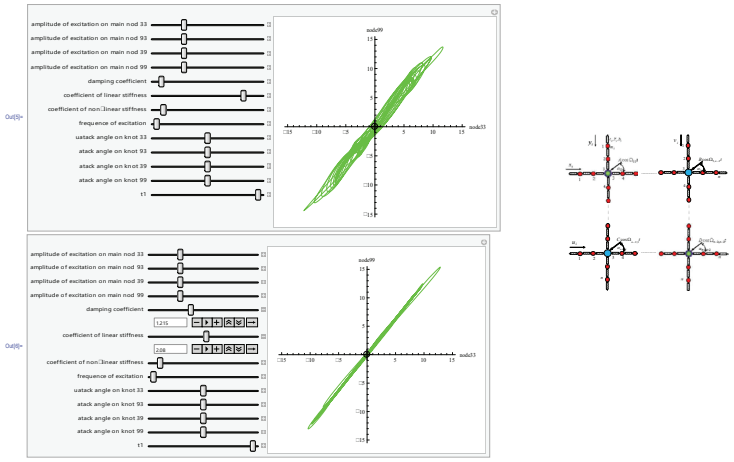

FIGURE 15. Synchronization attractors for opposite knots 33 and 99. External excitation acts on all four nodes.

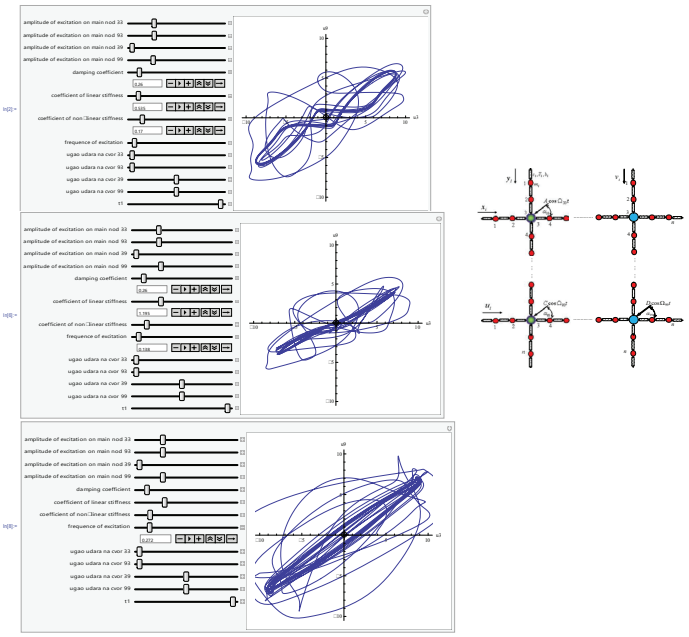

FIGURE 16. Synchronization attractors for knots from left vertical chain. External excitation acts on nodes 33, 93 and 99.

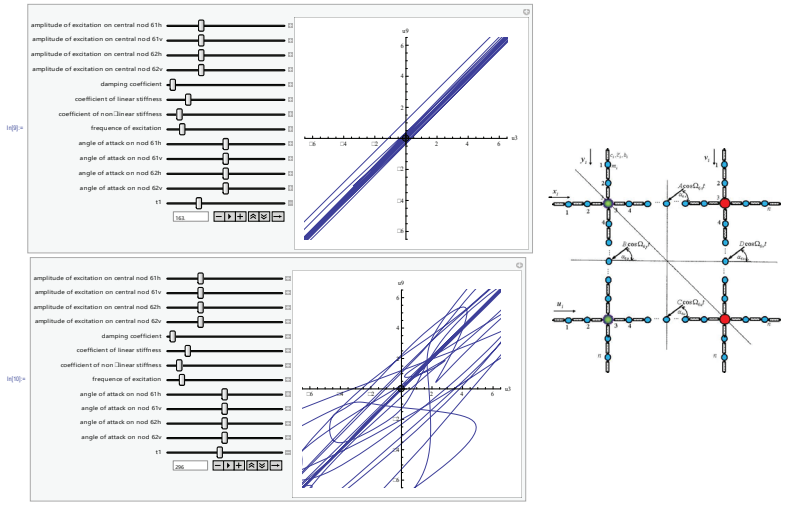

FIGURE 17. Synchronization of nodes on first vertical chain (nodes 33 and 39). External excitations act on middle dots in vertical and horizontal chains

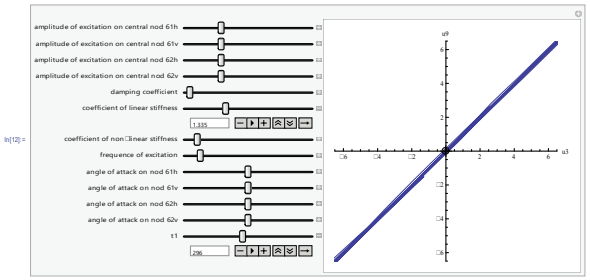

FIGURE 18. Identical synchronization of nodes on first vertical chain (nodes 33 and 39). External excitations act on middle dots in vertical and horizontal chains

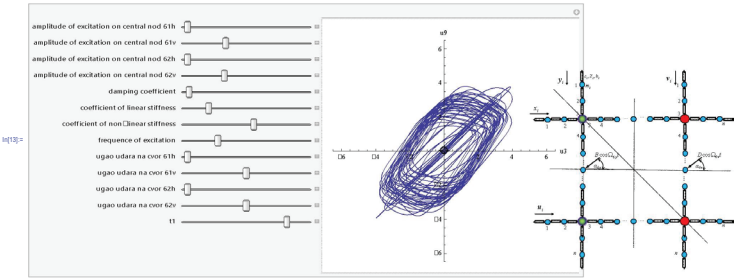

FIGURE 19. Identical synchronization of nodes on first vertical chain (nodes 33 and 39). External excitations act on middle dots in vertical chains

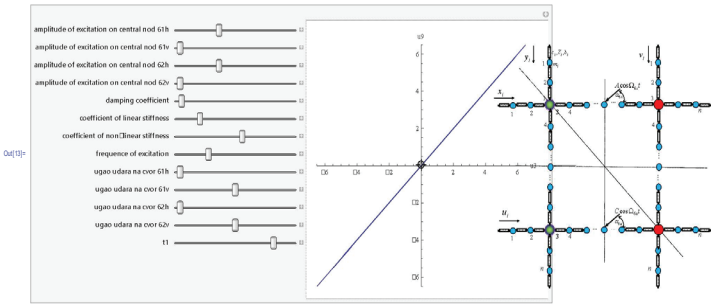

FIGURE 20. Identical synchronization of nodes on first vertical chain (nodes 33 and 39). External excitations act on middle dots in horizontal chains

When nodes from vertical chains share the signal from the external excitation that acts on the middle point of vertical chain, Fig. 19, then the initial identical synchronization is possible with transition to phase synchronization. If we retain all parameters on the same values and only change the position of the external excitations that acts on the middle points of the horizontal chains, Fig. 20, then we find out identical synchronisation of left vertical nodes. This is because excitation is symmetric in the latter case, and in the first case the influence of the signal from the parallel chains that has time delay causes the transition to phase synchronization.

The presented numerical simulation was performed to the identical synchronization mostly of the nodes from the left vertical chain, but all the given conclusions have relevance to synchronization of the other nodes.

4. Population model of bone remodelling

The accomplished knowledge of mathematical modeling of complex mechanical systems can be used for modeling of biological complex systems detecting the similar behavior in dynamics of system. Once the mathematical model has been established it is possible to analyze its dynamics by using multi-parametric analysis as suggested previously. The model in charge is the population model of bone cell time behavior under external periodic signal.

The system of bone cellular communication, which involves at least three main cellular lineages: forming-osteoblasts (OBs), resorbing-osteoclasts (OCs) and orchestrating-osteocytes (OCYs) cells lineage, with their self (autocrine signaling) and mutual (paracrine signalling) interactions and their interactions with the environment, is complex and elucidate a number of parameters that detail the psychological mechanism of bone tissue adaptation processes. One cycle of the bone regular turnover, so called bone remodeling, consists of the bone resorbing activity of the OCs and the bone forming activity of the OBs,

which are both driven by the signals transduced via OCYs from the external loading. The importance of this process goes with the fact that after every ten years of adult life the whole skeleton is regained and renewed due to this process. The following are the general form of models used by several authors [30–31] and references herein] representing the power of analytical approaches:

$$\frac{du_i}{dt} = \alpha_i f_i(u_i) + k \cdot f_i\big(u_i, \mu(t)\big) - \beta_i u_i \quad \text{for } i = 1,2,3$$

$$\frac{dz}{dt} = -k_1 v_1 + k_2 v_2 \text{ for } v_j = \begin{Bmatrix} u_j - \overline{u_j}, if\, u_j > \overline{u_j} \\ 0, if\, u_j \le \overline{u_j} \end{Bmatrix},\ j = 1,2 \tag{9}$$

where u_i are the densities of OCs, OBs and OCYs for $i = 1,2,3$, respectively, and $f_i(u_i)$ are the functions giving the growth rates which include the interaction between cell populations by the biochemical regulators in the form of power law approximation: $f_1(u_1, u_2) = u_1^{\gamma_{11}} u_2^{\gamma_{21}}$ and $f_2(u_1, u_2) = u_1^{\gamma_{12}} u_2^{\gamma_{22}}$, where $\gamma_{ij} f$ or $i, j = 1,2$ are defined by their autocrine and paracrine regulation. The last, so-called bone mass equation describes the activity of bone resorption and formation where z is total bone mass, k_i represents the normalized activities of bone resorption and formation, $\overline{u_i}$represents the steady states for the OCs and OBs and k is a positive proportionality constant measured in cells day^{-1}. The term $\mu(t)$ functions as a regulator of the bone-remodeling process and includes external signaling transduced via osteocyte activities that stimulates the production of OC and OB. This inputs function $\mu(t)$ can model regulators production from osteocytes as well as its regulation by the sclerostin inhibitor. An explicit functional form for $\mu(t)$ linked to osteocytes activity is was proposed in equation of osteocyte time changes as follow:

$$\frac{dS}{dt} = \underbrace{\alpha_1}_{OB\ embbeding\ rate} B^{\gamma_{31}(1+sin\,\theta t)} \left(1 - \frac{S}{K_s}\right)_+ + A(1 - cos\,\theta\, t) \tag{10}$$

where K_s is the osteocyte carrying capacity. The frequencies, θ, of the received and transduced signal are same in both functions but with some delay represented as phase shifting of π/2 or π in the following simulations. Many of the published bio/mathematical models represent only free dynamics of the bone cells although the evidence of external loading importance already widely exists. By presenting an experimentally evidenced mathematical model of bone, which includes externally forced turnover, we contribute to the realism of modelling. Critically, we approach the modelling through both deterministic (9) and (10), as though stochastic methods, which allow us to consider the intrinsic noisiness of the discrete process. We use a stochastic framework, Fig. 21., to simulate the creation and degradation, which encapsulates the noisy features of individual cell division and death [32–34].

FIGURE 21. Schematic diagram of how the next action in a stochastic simulation is calculated. The probabilities of all actions (creation and degradation of OC and OB, and/or OcY embedding) are calculated using the Law of Mass and Action and subsequently normalized to lie within [0, 1]. A uniformly random variable U is chosen between zero and one. Wherever this lies in the interval, this will choose the next action to occur, namely "Degradation of OC".

Using the proposed formalism from Fig. 21. we are able to extract the stochiometric creation and degradation relations for system (8), and present its probabilistic analogue:

$$u_i + u_j \xrightarrow{\alpha_i} 2u_i + u_j, u_i \xrightarrow{\beta_i} \emptyset, i = 1, 2, \dots, n \; and \; j \neq i. \tag{11}$$

System of Eqs. (9) for wo cell lineages, only forming OB and resorbing OC, has the following form:

$$\frac{du_1}{dt} = \alpha_1 u_1^{\gamma_{11}} u_2^{\gamma_{12}} - \beta_1 u_1 \tag{12}$$

$$\frac{du_2}{dt} = \alpha_2 u_1^{\gamma_{21}} u_2^{\gamma_{22}} - \beta_2 u_2 \tag{13}$$

$$\frac{dz}{dt} = -k_1 \, max[\,0, u_1 - \overline{u_1}] + k_2 \, max[\,0, u_2 - \overline{u_2}] \tag{14}$$

The unique nontrivial steady states of $\overline{u}_i$ could be calculated and in general depends on relations of eight different parameters involved in this simple example. The behavior of the solution of equations (12) and (13) can be explored by sign of the real part of the eigen values of Jacobian matric $J(\bar{u}_1, \bar{u}_2)$ of the steady state solutions. The nature of the Jacobian matrices' eigen value depends on the following functions:

$$trace\, J\left(\bar{u}_1, \bar{u}_2\right) = \psi = \beta_1\left(\gamma_{11} - 1\right) + \beta_2\left(\gamma_{22} - 1\right), \; \det J\left(\bar{u}_1, \bar{u}_2\right) = \Lambda = \beta_1\beta_2\left[\left(\gamma_{22} - 1\right)\left(\gamma_{11} - 1\right) - \gamma_{12}\gamma_{21}\right] = -\beta_1\beta_2\Pi$$
$$and \;\; \Delta = trJ^2 - 4\det J = \left[\beta_1\left(\gamma_{11} - 1\right) - \beta_2\left(\gamma_{22} - 1\right)\right]^2 + 4\beta_1\beta_2\gamma_{12}\gamma_{21}$$

The solution of system (12) and (13) exhibit limit cycle as ψ passes through 0 performing self-sustained oscillation of number of OC and OB, see Fig. 22 a). Also, if $\psi > 0 \; and \; \Lambda > 0 (\Pi < 0)$ solution yields unstable oscillations diverging away from the nontrivial steady state solutions $\overline{u}_i$ what defines existence of unstable source (repellers), see Fig. 22 c) and if $\psi < 0 \; and \; \Lambda > 0 (\Pi < 0)$ solution yields damped oscillations converging to the $\overline{u}_i$ what defines existence of stable attractors (sinks), Fig. 22 b). Likewise, if $\Delta < 0$ unstable saddle points can be find. The bifurcation diagram for these parameters could be designed

based on this analysis but more applicable solution for biologist is a tool where they can simultaneously change values of the parameters and track the shape of the phase diagram. In such a way find the combination of parameters value that satisfy desirable dynamics of solution. The multi-parametric analysis here is proposed where simply by moving sliders for parameter`s value we can follow the changes in the dynamics of the OC and OB, and find out the same inferences as it comes from structural analysis. (see Fig. 22).

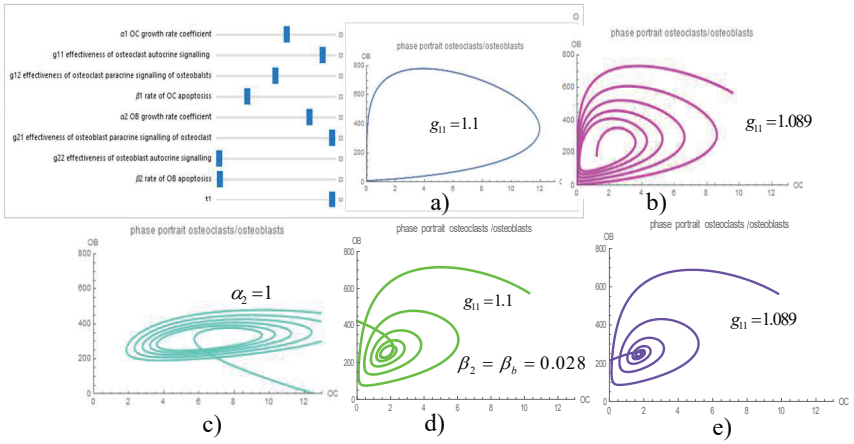

FIGURE 22. Phase portraits of OC-OB interaction dynamics for different γ_{11} parameter (effectiveness of osteoclast autocrine signaling) values: a) $\gamma_{11}=1.1$, b) $\gamma_{11}=1.098$; and c) $\alpha_2=1$, d) $\gamma_{11}=1.1$ and $\beta_2=\beta_b=0.028$ and e) $\gamma_{11}=1.098$ and $\beta_2=\beta_b=0.028$

The visualization of different system dynamics obtained by small changes of only one parameter (effectiveness of osteoclast autocrine signaling $\gamma_{11}=g_{cc}$)) are presented at Fig. 22. γ_{11}has been changed from the value of 1.1, Fig. 22 a) where the solutions exhibit limit cycle, also presented at [31], to the value 1.089, Fig. 22 b) where yielding damped oscillations converging to the nontrivial steady states $\overline{u_i}$ is presented. The values for the other parameter are: $\gamma_{12}=g_{cb}=-0.5,\gamma_{22}=g_{bb}=0,\gamma_{21}=g_{bc}=1$ are dimensionless parameters and $\alpha_1=\alpha_c=3,\alpha_2=\alpha_b=4,\beta_1=\beta_c=0.2,\beta_2=\beta_b=0.02$ have dimension day^{-1}. The following parameter`s range values are used in this research: $\gamma_{11}=g_{cc}\in(0;1.2),\gamma_{12}=g_{cb}\in(-1;0),\gamma_{22}=g_{bb}\in(0;1),\quad\gamma_{21}=g_{bc}\in(0;1),$ $\alpha_1=\alpha_c\in(0;5),\alpha_2=\alpha_b\in(0;5),\beta_1=\beta_c\in(0.1;0.5)$, $\beta_2=\beta_b\in(0.01;1)$. Initial conditions are constantly [OC(0); OB(0)]=(11; 231) in all simulations. However, having in mind the form of function Ψ it is obvious that changing, for instance value of parameter $\beta_2=\beta_b=0.028$ the response of the system dynamic no longer depend on the small changes of the value of $\gamma_{11}=g_{cc}$ with the same sensitivity, Fig. 22 e) and d). This is what underlines the importance of such a multi-parametric analysis presented herein. As an overall outcome, we can conclude that the right relation between parameters, not only value range of one primary parameter, is valuable

to be analyzed. This on the other side confirmed that continuous therapies that targeted only one parameter most likely would not be appropriate for a long-term period treatment.

It is possible to perform the changes of any parameter and even of all of them simultaneously with this procedure what is a very functional way of parameter`s ranges interpretation and explanation. By performing similar simulations with all involved parameters, it is straightforward to decide which of the parameter`s relation is the most influencing and most responsible for changes of model dynamics, even if the number of parameters or equations in the model enhanced. Obtained conclusions and discussions for parameter values and ranges are very applicable for the justification of effectiveness of mathematical models and their compliance with in-vivo experiments of bone cells. Nevertheless, it should bear in mind that the presented range of parameters for this paper are chosen only intuitively and the further readouts from in-vitro experiments could be extremely important in order to further validate the model. There also can be mentioned that known histopathological samples suggest limited number of cells per one cycle of remodeling what puts constraint to the maximal number of OC and OB present in the simulations, e.g., OC_{max} and $80 < OB_{max}$ per one cycle of bone remodeling. Parameters α_i and β_i are responsible for bounding the number of cells as they are cell`s growth and death rate coefficients. If the value of parameter $\alpha_2 = 1$ than it is obvious from the Fig. 22 c) that number of OB is bonded between 200 and 500 cells. However, using stochastic model Eq. (11) we perform cross-correlation analysis of parameter having in mind the mentioned variable constraints, the results are presented at Fig 23.

This allows probability that the transition number of cells, in the beginning and on the end of cycle, become small than 10 cells in which case predator-pray system yields to population extinction after only one cycle. Reasonably, our current research is the stochastic analogue Eq. (11) of the system of equations where we run 1000 simulations to explore these effects and perform cross-correlation simulation of parameters to find out appropriate intervals of expected value of parameters. Both the stochastics and deterministic trajectories can be found. Any individual stochastic trajectory does not match the deterministic solution. However, the average of these 1000 stochastic trajectories does correspond extremely well with the first peak of the deterministic solution, Fig. 24. The Fig. 24 presents benchmarking of the OC and OB time series obtained deterministically because of system (8) and with stochastic simulations form model (10). In a cycle of remodelling there is good agreement of results since the average trajectory of stochastic simulation absolutely corresponds to the deterministic solution, bottom diagrams of Fig. 24. However, in the next cycle, the population density is insufficient to start a stochastic process. This situation moves us further to the in/vivo/vitro experimental evidence that bone remodelling is not a self-sustained process rather it is strongly forced by an external signal.

This comparative analysis of different mathematical approaches shows that biological real event can be interpreted with a useful model depending on the different real constraints from the biological experiment. If the simulated population are large enough then the continuum deterministic approximation is appropriate, while if the population number tends to fall below 10 cells then the stochastic description is more apt.

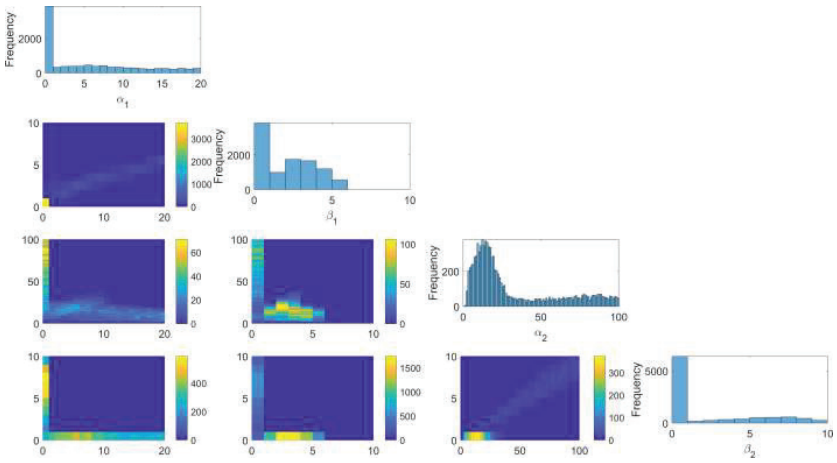

FIGURE 23. The cross-correlation simulations of the formation/degradation rate parameters. Specifically, a more yellow value suggests that the parameters are more likely to be chosen from this region of the parameters ranges. Four uniformly random variables from intervals: $\alpha_1 \epsilon [0; 20]$, $\beta_1 (\beta_2) \epsilon [0; 10]$ i $\alpha_2 \epsilon [0; 100]$ have been used to simulate the solutions of the Eq. (11). All accepted and presented solutions satisfy conditions: $OC_{max} < 20$, $80 < OB_{max} < 120$; $OB > 1$ after 1 day, and $OB < 5$ and $OC < 1$ for $t > 200$.

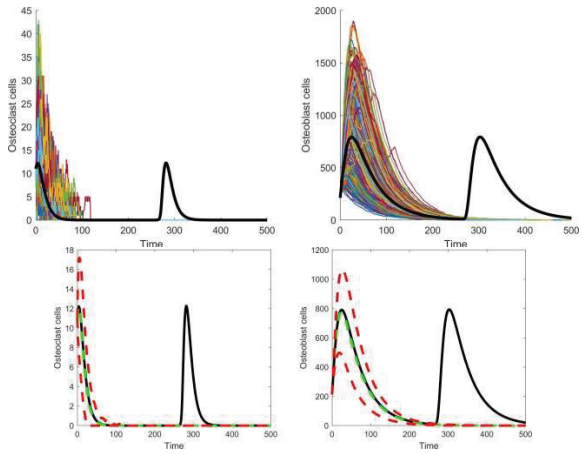

FIGURE 24. Top: 1000 stochastic simulations (colored lines, extinct after the first cycle) and 1 deterministic simulation (thick black line, periodically repeated) of the OB-OC model. Initial conditions are constantly (11; 212) in all simulations. Bottom: The black line is the same deterministic line illustrated in the top images. The green dashed line is the average trajectory extracted from the 1000 stochastic simulations. The red dashed lines show one standard deviation about the mean.

4.1. Non-Homogeneous model of bone cell population. If we include osteocytes OcY (Ss), OBs (Bs), OCs (Cs) and preosteoblastic (Ps) lineages of cells together with a bone mass equation the system (9) will be system of 5^{th} order ($n = 5$). Although parameter values exist in the literature, they are mainly approximate and are proposed to simplify and justify the model. Further, in all of the literature it is assumed that the γ_{ij} parameters are constant. However, in real bone remodelling processes the γ_{ij} parameters may depend on time and other factors. Unfortunately, these parameters cannot be directly measured and must be estimated. Thus, although initially we consider constant parameters (which simplifies the mathematical treatment and gives a high level of approximation but is useful as a benchmark for model validation), we later adapt the first equation of (9) to include the additional time dependant terms, which are based on the in-vitro experiment of loaded OcYs cell culture and adopt the Eq. (10) as system modification. The modification of the model was in editing the power term γ_{31} to time dependent oscillatory function $\gamma_{31}(1 + \sin(\theta t))$, which represents transduced signal of OcY, and inserting the mechanical periodic excitation $A(1 - \cos(\theta t))$ to the responding OcYs into the Eq. (10).

The simulation eventually stops, when $S = K_s$ because the term $(1 - S/K_s)_+$ evaluates to zero and all dynamics stop, which is highly artificial. However, going forward, we simply consider the production rate of S proportional to $(1 - S/K_s)$, whether positive or negative. This means that the number of OcY (S) is unrestricted, and the simulations are observed to have small oscillations around $K_s = 200$ cells per remodeling cycle (blue line on diagrams of Fig. 25 a)). Basically, this means that we assume there are a certain number of OcY ready to receive and send external signals and to open cell signaling channels in response to loading.

Many of the published bio/mathematical models represent only free dynamics of the bone cells although the evidence of external loading importance already widely exists. By presenting an experimentally evidenced mathematical model of bone, which includes externally forced turnover, we contribute to the realism of modelling. Critically, we approach the modelling through both deterministic and stochastic methods, which allow us to consider the intrinsic noisiness of the discrete process.

Starting from a set of homogeneous coupled ordinary nonlinear differential equations, and a biologically relevant set of parameter ranges, we are able to derive an analogous stochastic framework. Although the observed dynamics are similar, intrinsic noise produces fluctuations that drive the system toward more realistic descriptions of the process itself. Based on evidence from in-vitro experiments we incorporated both received and transduced signal as periodic rate transitions into the model (10). We find that the model can capture the essential autocrine, paracrine and synergistic characteristics of bone cell communication processes in response to the external incentives.

Specifically, including oscillatory signals with small delays between received and send a signal by OcY provides the closest matches between mathematical data and biology theory. This is straightforward to conclude from Fig. 25 c) where, after the period of resorption (the depression of the green line below zero), we observe a significant activation of osteoblasts that results in a formation period (the green line is

above zero). Comparing the green line in Fig. 25 c) with the green line in Fig. 25 a) (which has no over formation) we demonstrate that under the influence of the external periodic signal the local formation of the newly remodeled bone will exceed the amount of resorbed old bone. Furthermore, we investigated the relation between the strength of these two signals and got satisfactory results when the received signal has a smaller value of amplitude. This is our prediction from the model, which must be addressed experimentally. Namely, we require experiments that explore the magnitudes of information that OcY receives and explores. However, we showed that the steady-state value of total bone content changes depending on the external excitation and on the interplay of other parameters value that influences the dynamics of the process.

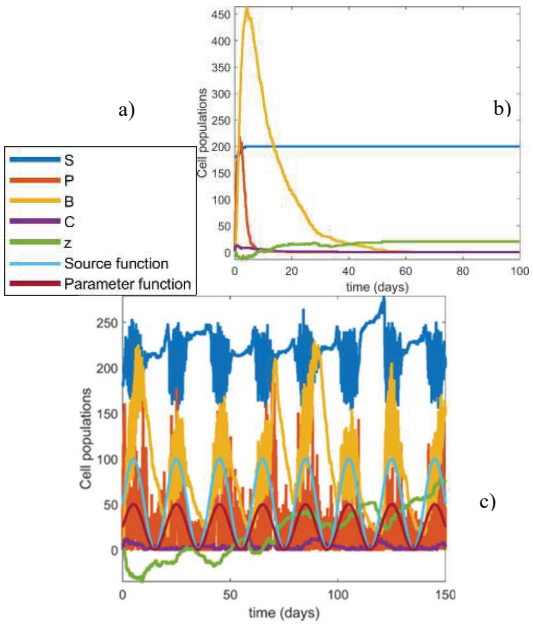

FIGURE 25. a) Legend for both figures. b) The number of osteocytes (OcY) is restricted to a maximum of 200 cells and diagram correspond to the same system of equations (1) of 5th order without external signaling. c) The number of OcY is unrestricted and has small oscillations around a number of 200 and external excitation to both the parameter and the source with a source strength is $A = 10$ and without delay.

How physical forces and changes in the mechanical properties of cells and tissues contribute to development, cell differentiation, physiology, and disease, in general, is a major interest of mechanobiology. Based on bone mechanobiology research, this research develops computational analytical models in order to address and better understand mechanotransduction - the molecular mechanisms by which bone cells sense and respond to mechanical signals. Downstream autocrine and paracrine

signaling in response to periodic excitation were modelled by cell population system of ordinary differential equations (9) to better represent and predict long-term behavior and consequences of bone cell loading. The system (9) is S-system (the generalized Lottka-Volterra system) and was solved deterministically together with its stochastic analog Eq. (11) (Gillespie algorithm [33]) used for noise check and system behavior dynamics analysis. Population dynamics are illustrated using time series plots, phase portraits, histograms and bifurcation diagrams. In-silico experimenting with a number of responding cells which is up to or around a certain threshold allows us to distinguish and describe different dynamics and relations between involved cells. The external signal can be considered as an additional term affecting the number of responding cells or as the functional periodicity of power low coefficients affecting autocrine signaling of forming cells. This research clearly shows the indispensability and beneficial effects of external excitation on balanced and regular bone cell activities and underline the importance of mathematical modeling and predictions.

5. Conclusion

The way to a mathematical model of the physical reality goes through establishing a conceptual model that contains numerous assumptions and approximations depending on what we want to explore as the dominant behavior of the physical reality. The first accepted assumption in the modeling of complex coupled deformable bodies was that the transversal displacements of middle plane (line) points of the bodies are small. We also assumed that there is no deplanation of the cross section of the bodies, we actually neglected shear deformations, that causes rotation between cross section and bending line so that we were able to apply Euler-Bernoulli theory. A general system of coupled partial differential equations of transversal oscillations for the system of coupled deformable bodies: plates, beams, membranes, and belts were established. On the base of the Bernoulli method first asymptotic approximation of the solutions were separated on the two domains. The space domain differs from body shape and boundary conditions, and the time domains have the same forms for any of the considered class of multi-body system dynamics. The completely analogy of system of coupled ordinary non-linear differential equations on time Eq. (4) of eigen time function in one amplitude mode is obvious for different physical coupled multi deformable body systems. Since there is mathematical analogy in structural model of different multi deformable body systems we conclude that there exists the phenomenological analogy too. This indicated mathematical analogy and phenomenological mapping are basis for extending results obtained in one research task of nonlinear dynamics of one mechanical system to the results of other mechanical systems. Since, we could obtain qualitative conclusions and explanations for dynamical behavior of mechanical systems with analog non-linear properties without solving them.

For the coupled plates with layer on rolling non-linear visco-elastic properties we approximately solved system of PDE`s (2) semi analytically in averaged asymptotic first approximation by using asymptotic method Krilov-Bogolyubov-Mitropoksiy.

Then we analyzed the stationary regimes of forced resonant non-linear oscillations for presented model of double plate system and introduced the analogy with system of beams, membranes and belts with the same coupling layer. These ideas were summarized form the results of numerous papers by Hedrih and Simonovic over several years [5–15–16], [6–8–24] and [9–26–27] and present the beauty of mathematical analytical calculus which could be the same even for physically different systems. The mathematical numerical calculus is a powerful and useful tool for making the final conclusions between too many input and output values. One step (part) of solutions were obtained numerically and presented at a series of first asymptotic approximations of the amplitudes-frequency characteristics of eigen time function modes in one amplitude mode. We could conclude that there exist complexities in the system forced non-linear response, depending on initial conditions and on proper relation between the system kinetic parameters.

In systems of coupled deformable bodies with layers of non-linear properties the non-linearity is source for appearing resonant jumps at the amplitude and phase -frequency curves of eigen time function modes in one amplitude mode in the resonant frequency interval. Between two jumps there appear three or five, or seven or more singular values of the stationary amplitudes and phases with alternatively stable and unstable values which build coupled singularities and trigger of coupled singularities, two stable values around one unstable stationary amplitudes and corresponding stable and unstable stationary phases. Passing through resonant ranges of the external excitation frequencies unique values of the stationary amplitudes and phases lose its stability and split into trigger of the coupled three singularities- two stable stationary values and one unstable saddle type of the amplitudes (or phases) for simple case without non-linear interactions between time modes. But, in the case when there are resonant interactions between modes, more than one pair of the resonant jumps appears, and there are possibilities for appearance of the coupled triggers of the coupled singularities consisting of odd number of the alternating coupled stable and unstable singularities. The mentioned instabilities of the stationary vibration regimes are associated with Hopf bifurcations in mathematical descriptions of the first asymptotic approximations of solutions. The described non-linear phenomena of passing through resonant regions are all characteristics in different deformable bodies systems with modeled non-linearity. The presented model from Ref. [9–17–26] of new features in interconnected layer introduced with rolling elements with its inertia of rolling without sliding and of translation of mass center is the novelty in modeling of the rheological elements. The presence of rolling elements in the interconnected layer introduces the part of the dynamic coupling into system of obtained PDE's. On the basis of the presented numerical comparison, we consequently conclude that dynamic coupling intensifies the phenomena of the resonant transition caused by the mutual interaction of the harmonics. The first asymptotic solutions for amplitude and phase changes (5) stand for transition changes in resonant regimes for a small time interval thus we can use them for analysis of local behaviour of system dynamics, that was presented in the section 2.1 and 2.1. However, the global behaviour of system dynamics play important role in many application and real consumption of construction. For

instance, identical synchronization (IS) can only be examined on long time scales and shows global dynamics possibilities of adjustment of system parts with an external signal. Once established IS can be changed by parameter alteration and there exists parameter regions that ensure conditions for IS even though the initial conditions of coupled dynamics can be different. To explore these parameters basin that gives IS it is suitable to use a multi-parametric analysis of the system based on the established mathematical model (4). That analysis was presented in chapter 2.4 and we concluded that for establishing IS the most sensitive parameter was the coefficient of damping coupling and we revealed the region of its values necessary for IS of deformable bodies. We also introduced the easiness of the new way to benchmark the influence of several parameters synchronously by using the proposed multi-parametric analysis.

Based on the research from the papers [18–29] that we summed up in section 3, which present also the application of the convenient multi-parametric analysis, we can underline several conclusions: In hybrid systems with static coupling, the increasing static coupling coefficient introduces better IS in a large region of the initial condition. But in systems with dynamic coupling, there exist attractor of synchronization but with a very large value of synchronization error which is in form of modal periodic function after the transition time, and also in systems with dynamical coupling the interesting phenomena of parameter ragged synchronization occur. For same parameter combination the IS repeats after specific time. and do not exist as global property of system dynamics.

The acquired knowledge and skills of complex system dynamics analysis using mathematical analogies can be applied also in mechanobiology. Several years of research in that filed has been realized by two postdoc research period supported by European Union trough ERASMUS MUNDUS and Marie Skłodowska-Curie Actions (MSCA) frameworks. Two projects were realized: six-month post PhD research period, between December 2015 and June 2016, at Interdisciplinary Centre for Mathematical and Computational Modelling of Warsaw University on subject of Bone Tissue Advanced Modelling with Piezoelectricity; and two-year, 2017-2019, post PhD research period at Biomedical Engineering Department, School of Engineering, Cardiff University under the project “Mathematical Modelling of Bone Externally Excited Remodelling” (MMoBEER). Bone mechanobiology research how mechanical forces and loadings influences architecture and quality of bone tissue and it is important to establish proper mathematical model of this process. Although it is possible to mechanically stimulate bone and quantify the tissue-level changes that occur, it is still extremely challenging to simultaneously delineate the cellular and molecular mechanisms that give rise to these changes.

Further, the complexity of the bone tissue processes and their interactions with the rest of the body limits the ability of a single biological in-vitro model to capture all of the relevant aspects of bone remodelling on all scales simultaneously what raise the degree of approximation of the model. Moreover, parameterization of an established accompanying mathematical model is difficult, given its dependency on the accuracy and availability of data. The available data from existing in-vitro experiments are the discrete values of measurable parameters that were taken

in defined cross points of readouts and cannot be enough to feed completely the continual model of mathematical equations. The models match in specific points but the lack of agreement in most of the time domain is present. For instance, the mathematical model can perform the behavior of the cells that have not yet been detected by biological experiments. The time scale of the in-vitro experiments depends on the viability of the cell population, in many cases during the controlled conditions of the experiment it is up to fourteen days, however, the cycle of the bone remodelling lasts up to 120 days, and mathematical model can give prediction even on the longer time scale. The important features of the credibility of biological models for in-vitro experiment depend on how well the accompanying mathematical models agree with results of repeatable experiments. The better agreement between theoretical mathematical models and experimental measurements often brings important advances and mutual benefits as better theories are developed. The established model has been presented in section 4 and among other we can summerised conclusion as following:

Introduces oscillatory signals with small delays between received and send signals by OcY, Eq. (10), provides the closest matches between mathematical data and biology theory. This is straightforward to conclude from Fig. 25 c) where, after the period of resorption (the depression of the green line below zero), we observe a significant activation of osteoblasts that results in a formation period (the green line is above zero). Comparing the green line in Fig. 25c) with the green line in Fig 25b) (which has no over formation) we demonstrate that under the influence of the external periodic signal the local formation of the newly remodelled bone will exceed the amount of resorbed old bone. We showed that the steady-state value of total bone content changes depending on the external excitation and also on the interplay of other parameters value that influences the dynamics of the process.

This collaboration between in-silico, mathematical, experiments and in-vitro, biological, experiments is inevitable for further success of the field. With this research, we wish to emphasize the importance, reliability and credibility of mathematical models are a great way of cementing biological intuition. Specifically, they provide causative mechanisms linking inputs and outputs and illuminating underlying assumptions that determine a biological system's dynamics. Finally, they offer a means of predicting new outcomes, as well as highlighting the most sensitive modelled components, resulting in the construction of new experimental hypotheses and experimentations that are more efficient.

Finally, mathematical modeling of complex systems and structures seeks not only under-standing and knowledge of mathematical calculus but also understanding and interpreting of the real phenomena that can be detected and measured in the dynamics of the investigated systems. The presence of the same dynamical behavior of the systems in disparate scientific field and application of mathematical analogies and mapping have significant contribution for any successful modeler. Further for systems with considerable number of involved parameters it is as important to explore the influence of the parameters on system dynamics as to discover mutual links between parameters. Bifurcation theory gives us possibilities to explore the influence of small changes of parameters on dramatic changes of dynamics of

system. However, multi-parametric analysis gives possibility to visualize and explore influence of several parameters synchronously. This is advantages for mathematical analysis but also for experimental setups in various scientific fields for acquiring adequate parameter's ranges.

Acknowledgment
This research was financially supported by the Ministry of Education, Science and Technological Development of the Republic of Serbia (Contract No. 451-03-9/2021-14/200109).

References

[1] M. Petrović, *Elementi matematičke fenomenologije, (Elements of mathematical phenomenology)*, Srpska kraljevska akademija, Državna štamparija Kraljevine Srbije, Beograd, 1911.
[2] M. Petrović, *Fenomenološko preslikavanje (Phenomenological Mapping)*, Srpska kraljevska akademija, Štamparija Planeta, Belgrade, 1933.
[3] D. Raškovoć, *Teorija oscilacija (Theory of oscillations)*, Naučna knjiga, 1965.
[4] K.R. (Stevanović) Hedrih, *Analogy between models of stress state, strain state and state of the body mass inertia mo-ments*, Facta Universitatis, Series Mechanics, Automatic Control and Robotics **1**(1) (1991), 105–120.
[5] K.R. (Stevanović) Hedrih, *Linear and nonlinear dynamics of hybrid systems*, Proceedings of the Institution of Mechanical Engineers, Part C: Journal of Mechanical Engineering Science **235**(20) (2021), 4535–4568. https://doi.org/10.1177/0954406220957699.
[6] K.R. (Stevanović) Hedrih, J.D. Simonović, *Structural analogies on systems of deformable bodies coupled with non-linear layers*, International Journal of Non-Linear Mechanics **73** (2015), 18–24. https://doi.org/10.1016/j.ijnonlinmec.2014.11.004.
[7] K.R. (Stevanović) Hedrih, J.D. Simonović, *Energies of the Dynamics in a Double Circular Plate Nonlinear System*, International Journal of Bifurcation and Chaos **21**(10) (2011), 2993–3011.
[8] K.R. (Stevanović) Hedrih, J.D. Simonović, *Multi-frequency analysis of the double circular plate system non-linear dynamics*, Nonlonesr Dynamics **67**(3) (2012), 2299–2315.
[9] J. Simonovic, *Dynamics and Stability of Dynamics Hybrid Systems*, Doctoral dissertation, University of Nis, Mechanical Engineering Faculty, (2012), 337.
[10] A. H. Nayfeh, *Nonlinear Interactions: Analytical, Computational and Experimental Methods*, Wiley, New York, 2000.
[11] K.R. (Stevanović) Hedrih, *Application of the Asymptotic Method for the Investigation of the Nonlinear Oscillations of Elastic Bodies - Energy Analysis of the Oscillatory Motions of Elastic Bodies*, Doctoral Dissertation, University of Niš, Serbia, 1975.
[12] Y. A. Mitropolyskiy, *Nelinyeynaya mehanika-Asimptoticheskie metodi*, Institut matematiki NANU Ukraini, Kiev, 1971.
[13] Y.A. Mitropolyskiy, N. Van Dao, *Lectures on Asymptotic Methods of Nonlinear Dynamics*, Vietnam National University Publishing House, Hanoi, 2003.
[14] K. R. (Stevanović) Hedrih, *The integrity of dynamical systems*, Nonlinear Analysis: Theory, Methods & Applications **63**(5–7) (2005), 854–871. https://doi.org/10.1016/j.na.2004.12.037.
[15] K.R. (Stevanović) Hedrih, *Energy analysis in a nonlinear hybrid system containing linear and nonlinear subsystems coupled by hereditary element*, Nonlinear Dynamics **51**(1–2) (2007), 127–140. https://doi.org/10.1007/s11071-007-9197-2.
[16] K.R. (Stevanović) Hedrih, *Energy transfer in double plate system dynamics*, Acta Mechanica Sinica **24**(3) (2008), 331–344. https://doi.org/10.1007/s10409-007-0124-z.
[17] J.D. Simonović, *Influence of rolling visco-elastic coupling on non-linear dynamics of double plates system*, Iranian Journal of Science and Technology, Transactions of Mechanical Engineering **39M1+** (2015), 163–173.

[18] J.D. Simonović, *Synchronization in Chains of Material Particles with Non-linear Features*, FME Transactions **42**(4) (2014), 341–345. https://doi.org/doi:10.5937/fmet1404341S.
[19] K.R. (Stevanović) Hedrih, A.N. Hedrih, *Eigen modes of the double DNA chain helix vibrations*, Journal of Theoretical and Applied Mechanics (JTAM) **48**(1) (2010), 219–231.
[20] A.N. Hedrih, K.R. (Stevanovic) Hedrih, B. Bugarski, *Oscillatory Spherical Net Model of Mouse Zona Pellucida*, Journal of Applied Mathematics & Bioinformatics **3**(4) (2013), 225–268. https://doi.org/3af0996a052823809e86172fa4bfdd6e.pdf.
[21] A.N. Hedrih, *Modelling oscillations of Zona Pellucida before and after fertilization*, ENOC Young Scientist Prize, Paper. EUROMECH Newsletter, (2011), 6–14.
[22] K. R. (Stevanovic) Hedrih, J. D. Simonović, *Dynamical Absorption and Resonances in the Sandwich Double plate System Vibration with Elastic layer*, Scientific Technical Review **2** (2007), 1–10.
[23] O.A. Goroško, K.R. (Stevanović) Hedrih, *Analitička dinamika (mehanika) diskretnih naslednih sistema, (Analytical Dynamics (Mechanics) of Discrete Hereditary Systems)*, *University of Niš, 2001.*
[24] K.R. (Stevanović) Hedrih, J.D. Simonović, *Non-linear dynamics of the sandwich double circular plate system*, Int. J. Non. Linear. Mech. (2010), 902–918.
[25] K.R. (Stevanović) Hedrih, J.D. Simonović, *Transversal Vibrations of a non-conservative double circular plate system*, Facta Universitatis Series Mechanics, Automatic Cointrol and Robotics **62**(1) (2012), 40–54.
[26] J.D. Simonović, *Dynamics of Mechanical Systems of Complex Structure*, Magister of Science Thesis, University of Nis, Serbia, 2008.
[27] K.R. (Stevanović) Hedrih, *Modes of the homogeneous chain dynamics*, Signal Processing **86**(10) (2006), 2678–2702. https://doi.org/10.1016/j.sigpro.2006.02.031.
[28] J.D. Simonović, *Synchronization in Coupled Systems with Different Type of Coupling Elements*, Differntial Equations and Dynamical Systems **21**(1) (2013), 141–148. https://doi.org/https://doi.org/10.1007/s12591-012-0130-x.
[29] P. Pivonka, S.V. Komarova, *Mathematical modeling in bone biology: From intracellular signaling to tissue mechanics*, Bone **47**(2) (2010), 181–189. https://doi.org/10.1016/j.bone.2010.04.601.
[30] J.D. Simonović, *Simultaneous multi-parametric analysis of bone cell population model*, In: W. Lacarbonara, B. Balachandran, J. Ma, J.A. Tenreiro Machado, G. Stepa, (ed.), *New Trends Nonlinear Dyn.*, Proceeding, Springer Nature Switzerland AG (2020), 233–241.
[31] J. Belmonte-Beitia, T.E. Woolley, J.G. Scott, P.K. Maini, E.A. Gaffney, *Modelling biological invasions: Individual to population scales at interfaces.* Journal of theoretical biology **334** (2013), 1–12. https://doi.org/10.1016/j.jtbi.2013.05.033.
[32] D.T. Gillespie, *Stochastic simulation of chemical kinetics*, Annual review of physical chemistry **58** (2007), 35–55. https://doi.org/10.1146/annurev.physchem.58.032806.104637.
[33] N.G. van Kampen, *Stochastic processes in physics and chemistry*, Amsterdam, 1992.